

## Supplement Material

### Supplemental Methods

#### **Ethics**

Studies complied with the principles stated in the “*Declaration of Helsinki*” and were covered by approval (06/Q2001/197) from Bath Research Ethics Committee. Patients gave written informed consent to be recruited in the study.

Experiments involving live animals were performed in accordance with the *Guide for the Care and Use of Laboratory Animals* (the Institute of Laboratory Animal Resources, 1996) and with approval of the British Home Office and the University of Bristol.

#### **Isolation and culture of pericyte progenitor cells**

Pericyte progenitor cells (SVPs) were isolated from vein leftovers of patients undergoing coronary artery bypass graft surgery as described earlier.<sup>1</sup> In brief, saphenous veins, collected in PBS containing penicillin and streptomycin, were carefully dissected from surrounding tissues using a sterile scalpel and then thoroughly washed in abundant PBS, containing antibiotics. Veins were then manually minced with a scalpel before being incubated for 4 hours with 3.7mg/mL Liberase 2 (Roche). The remaining aggregates were eliminated by passing the cell suspension through 30µm cell strainer. Cells were then incubated with anti-CD31 conjugated beads (Miltenyi) and passed through a magnetic column, following manufacturer’s instruction. This allowed efficient removal of mature endothelial cells. After depletion of CD31 positive cells, remaining cells were further incubated with anti-CD34 beads (Miltenyi) for 30min at 4°C and then processed to obtain purified CD34 positive cells. Sorted cells were plated on fibronectin (10µg/mL) coated plates in presence of differentiation medium (EGM2-2% FBS, Lonza). Adherent cells appeared 5-10 days later which were fed every three days with fresh medium and passaged to new culture dishes once they reached 60-70% confluence. Trypsin-EDTA (Invitrogen) was utilized to detach cells from the growth substrate. For *in vitro* and *in vivo* experiments, cells were used at passage 7.

#### **Flow cytometry analysis**

SVPs were stained for surface antigen expression using combinations of the following antibodies: anti-CD90, anti-CD-105, anti-CD34, anti-CD31, anti-CD45 (all from BD biosciences), anti-CD14 and anti-CD16 (both from Invitrogen) After staining, fluorescence was analyzed using a FACS Canto II flow cytometer and FACS Diva software (both BD Biosciences, UK). To control for specificity, an aliquot of cells was stained with secondary antibody only.

#### **Isolation of circulating mononuclear cells and bone marrow mesenchymal stem cells**

Mesenchymal stem cells were isolated from the bone marrow of the patients undergoing hip joint replacement.  $1.0 - 1.5 \times 10^7$  BM-MNCs were resuspended in 10 mL of MSCGM Single Quots medium (Lonza) and plated in a T-25 cm<sup>2</sup> flask for 7-10 days. The resulting mesenchymal stem cells (MSCs) were adherent to plastic, positive for surface antigen markers such as CD90, CD105 and CD73 and negative for CD45, CD34 and CD14. *In vitro*, MSCs were able to differentiate into osteoblasts, adipocytes and chondroblasts. Cells were used at 4<sup>th</sup> passage for *in vivo* studies.

#### **Isolation and culture of rat adult cardiomyocytes**

Male Wistar rats were killed by cervical dislocation, the heart dissected and rinsed in cold solution A containing (in mM): 137 NaCl, 5 KCl, 1.2 MgSO<sub>4</sub>, 1.2 NaH<sub>2</sub>PO<sub>4</sub>, 20 N-hydroxyethylpiperazine-N’ -2-ethanesulphonic acid (HEPES), 16 glucose, 5 Na pyruvate and 1.8 MgCl<sub>2</sub> (pH 7.25 with NaOH) + 0.75 mM CaCl<sub>2</sub>. The heart was cannulated via the

aorta and perfused for 4 min with solution A + 0.75 mM CaCl<sub>2</sub> (all perfusing solutions were oxygenated and maintained at 37 °C). This was followed by a 4-min perfusion with solution A + 0.09 mM ethylene glycol-bis (β-aminoethyl ether) N,N,N',N'-tetraacetic acid (EGTA). Next the heart was digested with 50 ml of enzyme solution containing: solution A + 0.09 mM EGTA, 50 mg collagenase (Worthington Biochemical Corporation, Lakewood, New Jersey, USA. Type I), 5 mg protease (Sigma, Poole, Dorset, UK. Type IV), with (glutamate loaded) or without (control) 6.4 mM potassium L-glutamate until the tissue felt soft. There was a final 4-min perfusion with solution A + 0.15 mM CaCl<sub>2</sub> before the ventricles were cut down and sliced. The sliced ventricles were suspended in approximately 20–25 ml solution A + 0.15 mM CaCl<sub>2</sub> and shaken for 6 min at 37 °C. After filtration, cells were allowed to sediment, the supernatant was discarded, and the remaining cell layer suspended in solution A + 0.5 mM CaCl<sub>2</sub>. This sedimentation, removal of supernatant and resuspension step was repeated, but this time the cells were suspended in solution A + 1 mM CaCl<sub>2</sub>. This technique typically produced a yield of over 90% rod-shaped cells with the ability to exclude Trypan Blue.<sup>2</sup> The resulting cells were then washed repeatedly with medium 199 (Invitrogen) supplemented with 0.2% BSA, 10% FBS, 5 mM creatine, 5 mM taurine, 2 mM carnitine, 10 μM cytosine-D-arabinofuranoside (all from Sigma chemicals), ITS and antibiotics (both from Invitrogen). After the final wash cells were resuspended in the same medium and plated on laminin coated culture dish according to the experiments.

#### ***Isolation and culture of adult mouse cardiac fibroblasts***

Adult fibroblasts were isolated by the principle of selective plating as previously described, with some minor modifications. In brief, ventricles from 8 weeks old male CD1 mice (Harlan, UK) were minced and digested twice for 10 min with 1000U Collagenase Type 1 (Worthington), followed by 9500 U Collagenase Type 2 (Worthington) for 70 min. Red blood cells were lysed with a standard ammonium chloride/EDTA buffer and the resulting suspension was plated for 1 h in cell culture dishes in DMEM/10% FBS/1% Penicillin-Streptomycin. The cultures were washed thoroughly with PBS and the remaining adherent cells were cultivated for 3 days without signs of myofibroblast differentiation. Cells were passaged once confluent and used for the experiments. For differentiation experiments, fibroblasts were treated with Angiotensin II (100nM) for 24h in a 8-well chamber slide, followed by immunocytochemical staining for α-smooth muscle actin and methyl CpG binding protein 2 (MeCP2) to confirm its differentiation in to myofibroblasts.<sup>3</sup>

#### ***Mouse model of myocardial infarction and SVP transplantation***

Myocardial infarction (MI) was induced in 8 weeks-old immune deficient CD1-FOXO<sup>nu/nu</sup> (Charles River) or immune competent CD1 (Harlan) by permanent ligation of the left anterior descending coronary artery (LAD) as described.<sup>4, 5</sup> In brief, with mice under anesthesia (2,2,2 tribromo ethanol, 0.3gm/kg, i.p.) and artificial ventilation, the chest cavity was opened and, after careful dissection of the pericardium, LAD was permanently ligated using a 7-0 silk suture. This was followed by injection of Dil-stained SVPs (3X10<sup>5</sup> or 1X10<sup>6</sup>, 7<sup>th</sup> passage), MSCs (1X10<sup>6</sup>, 4<sup>th</sup> passage) or phosphate buffered saline (PBS) at 3 different sites along the infarct border zone with final volume of 10μL at each site. Animals were allowed to recover with aseptic precautions and received analgesic medication (Buprenorphine, 0.1mg/kg s.c.) to reduce post-operative pain. Sham operated animals underwent a similar procedure without LAD ligation.

#### ***Effect of miR-132 antagonism on SVP reparative activity in vivo***

To investigate the importance of miR-132 in SVP-induced promotion of post-MI recovery, SVPs were transfected with anti-miR-132 (50nmol/L) or scramble sequence (50nmol/L, both from Applied Biosystems, UK) for 48h using commercially available transfection agent Lipofectamine 2000 (Invitrogen, UK). After 48h, SVPs were trypsinized, labelled with Dil and transplanted into mouse infarcted heart (3 X 10<sup>5</sup> cells/animal). Effective antagonism of miR-132 was tested *in vitro* and *in vivo* by RT-PCR and western blotting for target gene p120RasGAP.

### ***Echocardiography and hemodynamic measurements***

Measurements of dimensional and functional parameters were performed before and at different time points after MI using a high-frequency, high resolution echocardiography system (Vevo 770, Visual Sonics, Toronto, Canada) (n=at least 6 mice per group). Briefly, mice were anesthetized using tribromo-ethanol and transferred to an imaging stage equipped with a warming pad for controlled maintenance of mouse body temperature at 37°C and a built-in electrocardiography system for continuous heart rate (HR) and respiratory rate monitoring. The thickness of the left ventricle (LV) was measured at the level of the papillary muscles in parasternal short axis at end-systole and end-diastole. LV ejection fraction (LVEF) and fractional shortening (LVFS) were determined as described by De Simone *et al.*<sup>5-7</sup> Following the final echocardiography measurement, under anaesthesia, intraventricular pressure measurement was done using a high-fidelity 1.4F transducer tipped catheter (Millar Instruments, Houston, TX, USA) inserted into the left ventricle through right carotid artery (n=at least 6 per group). The position of transducer into the heart was confirmed by the rapid deflection of the diastolic pressure wave without any change in systolic pressure. After 5min stabilization, baseline data were collected, including the HR, Peak LV systolic pressure (LVESP), LV end-diastolic pressure (LVEDP), and maximal rates of LV pressure rise ( $dP/dt_{max}$ ) and fall ( $dP/dt_{min}$ ).<sup>5, 7, 8</sup> To calculate pressure volume relationship, the recording from Millar catheter was synchronized with echocardiography measurements as per manufacturer instructions.<sup>4, 5, 7</sup>

### ***Measurement of blood flow using fluorescent microspheres***

Myocardial perfusion was measured using fluorescent microspheres (n= at least 6 mice per group). A polyethylene (PE10) catheter was inserted through the right carotid artery for the reference blood withdrawal. Microspheres, 0.1µm in diameter (Molecular Probes, Invitrogen) were injected into the LV cavity over 1min and flushed with 0.15ml of 0.9% NaCl. Reference blood was collected *via* the carotid catheter starting 15sec before to 1min after the microsphere injection. The animals were sacrificed 2min later and the heart was removed and separated into LV and right ventricle (RV). The kidneys were also collected and analyzed as internal control organs to demonstrate homogenous distribution of the microspheres throughout the bloodstream. Each sample was weighed, cut into small pieces and digested in 10ml of 2M ethanolic KOH containing 0.5% Tween 80 at 60°C for 48h with constant shaking. After complete digestion of tissues, the microspheres were collected by centrifugation at 2,000 x g for 20min and sequential washing with 10ml of deionized water with or without 0.25% Tween 80. Finally, microspheres were dissolved in 3ml of 2-ethoxyethylacetate and the fluorescence intensity was determined using a fluorophotometer (Fluostar Optima, BMG labtech). Regional blood flow was calculated as the absolute blood flow in ml/min/g of tissue as described earlier.<sup>5, 7, 9</sup>

### ***Measurement of vascular permeability***

In vivo myocardial vascular permeability was measured using modified fluorescent labeled dextran method (n= 6 mice per group). FITC-labeled 70kD dextran was injected intravenously followed 5min later by TRITC-labeled dextran. Mice were sacrificed 30sec from last injection. Cardiac tissue was dissected, homogenized and the fluorescence of the supernatant measured using fluorophotometer (Fluostar Optima, BMG labtech). The amount of TRITC-labeled dextran was subtracted from the amount of FITC-labeled dextran, to correct for the intravascular space and give the total amount of extravasated dextran.

### ***Biochemical measurements***

To verify the impact of cell therapy of neurohormonal activation after MI, angiotensin II (Ang II) and norepinephrine (NE) levels in plasma and LV myocardium were measured using commercially available ELISA kits (SPI bio and IBL international respectively).<sup>10</sup> The expression of Ang II receptor, type 1 (AT1R) was quantified by western blot (*vide infra*).

## **Immunohistochemistry**

### *Whole mount sections preparation*

After completion of hemodynamic measurements, hearts were stopped in diastole by intramyocardial injection of cadmium chloride. Hearts were then washed free of blood by retrograde perfusion with PBS-2% EDTA solution, followed by fixation with freshly prepared ice-cold 4% paraformaldehyde (PFA) solution under physiological pressure from abdominal aorta. Hearts were immediately cut in to 5mm-thick cross sections and embedded in tissue tech O.C.T compound for cryosectioning. Cryosections were made at 60µm thickness, placed on superfrost *ultra plus* (Thermo, UK) slides, air dried for 30min and stored in -80°C till immunostaining. In some experiments, animals received an intravenous injections of biotinylated isolectin-B4, and after 10min hearts were stopped in diastole, perfused and processed as above.

### *Graft Localization and characterization*

We used whole mount sections for localization and characterization of injected SVPs at day 5, 14 and 42 post-MI. Sections, were post-fixed with acetone at -20°C for 10min and air dried at room temperature for 30min. Following permeabilization with 1% triton-X 100 and blocking of non-specific antigens, sections were incubated overnight at 4°C with biotinylated isolectin-B4 to stain endothelial cells (1:50, Invitrogen, UK), followed by incubation with streptavidin Alexa Flour 488 (1:100, Invitrogen, UK) for 3h at room temperature. To characterize the injected SVPs, some sections were subjected to secondary staining by overnight incubation with pericytes markers NG2 (1:100, mouse monoclonal, Millipore) or PDGFβR (1:100, rabbit polyclonal, Santa Cruz, USA), followed by Alexa Flour goat anti mouse or rabbit (1:100, Invitrogen, UK). Serial z-stack images of myocardium were generated using Leica SP5 AOBS confocal laser scanning microscope (Wolfson Bioimaging facility, University of Bristol).

### *Vascular density profiling*

For capillary density, 5µm thick LV cryosections were incubated with biotinylated Isolectin B4 (Invitrogen, UK, 1:50, 2h at 37°C in a humidified chamber), followed by streptavidin Alexa Fluor 488 (Invitrogen, UK, 1:100, 1h at room temperature). For arteriole density, same sections were probed with anti-mouse α-smooth muscle cell actin antibody conjugated with Cy3 (Sigma chemicals, UK, 1:400, 1h at room temperature). To recognize cardiomyocytes, sections were also stained with mouse monoclonal primary antibody for the cardiomyocyte marker α-sarcomeric actin (Abcam, UK, 1:100, overnight at 4°C), which was revealed by counterstaining with the secondary antibody conjugated to Alexa 568 (Invitrogen, UK, 1:100, 1h at room temperature). Capillaries and arterioles were calculated in at least 20 fields at X200 magnification and the final data expressed as the number of capillaries or arterioles per square millimetre. Arterioles were also categorized according to their luminal size.<sup>4, 11</sup>

### *Analysis of inflammation*

For analysis of inflammatory cells, 5µm serial cryosections were incubated overnight with polyclonal VEGF-B antibody (Abcam, UK, 1:100) followed by Goat anti-rabbit Alexa Flour 488 antibody (Invitrogen, UK, 1:100). Same sections were then probed with either mouse monoclonal CD45 antibody (BD Biosciences, UK, 1:40) or rat anti-mouse Mac-3 antibody (BD Biosciences, UK, 1:40) overnight, followed by goat anti-mouse Alexa Flour 568 antibody (Invitrogen, UK, 1:100).

### *Proliferation and apoptosis*

For analysis of proliferation, sections were incubated overnight with mouse monoclonal PCNA antibody (BD Biosciences, UK, 1:100), followed by goat-anti mouse secondary antibody conjugated with Alexa Flour 488 (Invitrogen, UK, 1:100). Injected SVPs were identified by their Dil staining. The data were expressed as percentage of PCNA<sup>pos</sup> Dil<sup>pos</sup> SVPs. To identify the proliferating endothelial cells, after staining with PCNA, sections were stained with isolectin-B4 as described above.

Cardiomyocytes and endothelial cells apoptosis was quantified on LV cryosections (5µm) by the terminal deoxynucleotidyltransferase (TdT)-mediated dUTP nick-end labeling (TUNEL) technique (in situ cell death detection kit Fluorescein, Roche applied science,



USA). Following treatment of slides with proteinase K (20µg/ml, 30min at 37°C), TUNEL assay was performed according to the manufacturer's instruction. Same sections were then stained with DAPI to recognize nuclei. Cardiomyocytes and endothelial cells were stained as described above. Twenty fields were randomly evaluated in each section at X400 magnification. The fraction of TUNEL positive nuclei over total cardiomyocyte or endothelial cell nuclei was then calculated.<sup>5, 12</sup>

#### *Identification of p120RasGAP expression in myocardium*

For identification of p120RasGAP, 5µm cryosections were incubated overnight with monoclonal p120RasGAP antibody (SantaCruz, USA, 1:50) followed by Goat anti-mouse Alexa Flour 488 antibody (Invitrogen, UK, 1:100). Same sections were then probed with biotinylated Isolectin B4 (Invitrogen, UK, 1:50) to identify the endothelial cells or α-sarcomeric actin (Abcam, UK, 1:100) to identify cardiomyocytes or s100A4 (Abcam, UK, 1:50) to identify fibroblasts. To understand the distribution of p120RasGAP in the myocardium, multiple low magnification images (50X) were captured using Leica SP5 AOBs confocal laser scanning microscope (Wolfson Bioimaging facility, University of Bristol), and then merged together using Volocity imaging software. For identification of the type of cells expressing p120RasGAP, images were captured.

#### *Identification of cardiac stem cell pool in myocardium*

For identification of cardiac stem cell pool in the myocardium, 5µm paraffin sections were incubated with rabbit polyclonal GATA4 antibody (SantaCruz, USA, 1:40, 2h at 37°C, followed by donkey anti-rabbit Alexa Flour 555 antibody (Invitrogen, USA, 1:800)), goat polyclonal c-Kit antibody (R&D, USA, 1:50, 2h at 37°C, followed by donkey anti-goat Alexa Flour 488 antibody (Invitrogen, USA, 1:400)), mouse monoclonal mast cell tryptase (Abcam, USA, 1:50, 2h at 37°C, followed by donkey anti-mouse Alexa Flour 555 antibody (Invitrogen, USA, 1:800)) and mouse monoclonal α-sarcomeric actin (Sigma Chemicals, Italy, 1:100, 1h at 37°C, followed by donkey anti-mouse DYLight 649 antibody (Invitrogen, USA, 1:400)). Proliferating c-Kit cells were identified using rabbit monoclonal Mcm-5 antibody (Abcam, USA, 1:100, over night incubation at 4°C, followed by donkey anti-rabbit Alexa Flour 555 antibody, Invitrogen, USA, 1:800)

#### *Assessment of myocardial fibrosis*

Myocardial fibrosis was analyzed by Azan Mallory<sup>4</sup> or Sirius red<sup>7</sup> staining followed by morphometric analysis using the Image Pro analysis software (MediaCybernetics, USA) and the data were expressed as the percentage of scar size or fibrotic area.

#### *Assessment of calcification*

Myocardial calcification was assessed using Von Kossa staining as described earlier.<sup>13</sup> In brief 5µm cryosections were incubated with 1% silver nitrate solution and exposed to ultraviolet light for 60 minutes. After serial washes with distilled water, un-reacted silver was removed with 5% sodium thiosulfate for 5 minutes and finally counterstained with nuclear fast red. Images were obtained using Olympus light microscope fitted with camera. Three weeks old mice fibula was used as positive control.

#### ***Immunocytochemistry***

For immunocytochemical analysis of SVPs and cardiac fibroblasts, cells were fixed with freshly prepared 4% PFA after different treatment protocols. SVPs were probed with with one of the following antibodies – pericytes markers NG2 (1:100, Millipore, UK) and PDGFRβ (1:100, Santa Cruz, USA). Furthermore, in differentiation assays, cells were analysed for expression of cardiomyocytes marker α-sarcomeric actin (1:100, Abcam, UK), and connexin-43 (1:3000, Sigma Chemicals, UK), cardiac transcription factor GATA-4 (1:20, Santacruz, USA), vimentin (1:20, Abcam, UK) and α-smooth muscle actin (1:400, Sigma Chemicals, UK). Cardiac fibroblasts were probed with α-smooth muscle actin (1:400, Sigma Chemicals, UK) or MeCP2 (1:200, Abcam, UK).

#### ***RNA isolation and quantitative RT-PCR***

Total RNA was extracted from flash-frozen LV samples (Trizol, Invitrogen, UK), SVPs, SVP-CM or HUVECs using Trizol according to the manufacturer's instructions.

One microgram of total RNA was reverse transcribed using qiagen reverse transcriptase kit, followed by amplification of cDNA using quantitect primers for vascular endothelial growth factor (VEGF)-A, VEGF-B, VEGF-C, CX3CR1, platelet derived growth factor- $\beta$  receptor (PDGFR $\beta$ ), angiopoietin, NG2, CD40, CD80, Fas Ligand and internal control 18S (all from Qiagen, UK).

For analysis of miR-132, 10ng of total RNA was reverse transcribed using TaqMan reverse transcriptase kit and specific reverse transcription primers for miR-132 and internal control RNU6B (all from Applied Biosystems, UK). Amplification of cDNA was performed using TaqMan universal PCR mix kit (Applied Biosystems, UK) in Light Cycler 480 (Roche, UK).

For quantification, the amount of RNA/miRNA was normalized to the amount of 18S/U6 miRNA using the 2- $\Delta\Delta$ CT method. Each reaction was performed in triplicate.<sup>14</sup>

### **Protein extraction, western blotting and ELISA**

Proteins were extracted from LV, SVPs or HUVECs using ice-cold RIPA buffer. Protein concentration was determined using the Bio-Rad protein assay reagent (Bio-Rad, UK). Detection of proteins by western blot analysis was done following separation of whole tissue / cell extracts (50 $\mu$ g) on SDS-polyacrylamide gels. Proteins were transferred to polyvinylidene difluoride membranes (PVDF, Amersham-Pharmacia, Germany) and probed with the following antibodies: Ser473- phospho-Akt (Cell Signaling, UK, 1:1000), Akt (Cell Signaling, UK, 1:1000), pGSK3beta (Cell Signaling, UK, 1:1000), GSK3beta (Cell Signaling, UK, 1:1000), Ser 1177-phospho-eNOS (Cell Signaling, UK, 1:1000), eNOS (Cell Signaling, UK, 1:1000), Thr 202/Tyr 204- phospho-Erk1/2 (Cell Signaling, UK, 1:1000), Erk1/2 (Cell Signaling, UK, 1:1000), Ser112- phospho-Bad (Cell Signaling, UK, 1:1000), Bad (Cell Signaling, UK, 1:1000), Bcl-2 (Cell Signaling, UK, 1:1000), cleaved-caspase-3 (Cell Signaling, UK, 1:1000), Ser 133-phospho CREB (Cell Signaling, UK, 1:1000), CREB (Cell Signaling, UK, 1:1000), p120RasGAP (SantaCruz, USA, 1:500) and Angiotensin type II receptor 1 (SantaCruz, USA, 1:500). Actin (Cell Signaling, UK, 1:1000) was used as loading control. For detection, secondary antibody goat anti-rabbit or anti-mouse or donkey anti-goat conjugated to horseradish peroxidase (all from Santacruz, USA 1:5000) were used, followed by chemiluminescence reaction (ECL, Amersham Pharmacia, Germany). Density of the bands was analyzed using Image-J (NIH, USA) software and data expressed as fold changes.<sup>4,7</sup>

ELISA were performed with 25 $\mu$ g of total protein using the antibodies against VEGFA, VEGFB<sub>186</sub>, VEGFC and angiopoietin-1 using standard ELISA protocol. For ELISA with CM (*vide infra*), 100 $\mu$ l of total CM was used.

### **In vitro Experiments**

#### *Hypoxia-starvation and sample collection*

For hypoxia-starvation experiments, SVPs were serum starved for 8h followed by exposure to 1% O<sub>2</sub> for 18h. At the end of hypoxia, conditioned supernatant medium was collected from SVPs for further experiments (*vide infra*). Cells were then used for measurement of caspase-3/7 activity using caspase-glo assay (Promega, UK) or protein and RNA extraction.

#### *In vitro inhibition of miR-132*

For the inhibition of miR-132 in vitro, SVPs were transfected with anti-miR-132 (50nmol/L) or scrambled sequence (50nmol/L, both from Applied Biosystems, UK) using commercially available transfection agent Lipofectamine 2000 (Invitrogen). Forty eight hours later, cells were exposed to hypoxia/starvation and sample collected for measurement of caspase activity, protein and RNA analysis and BRDU incorporation assay as below.

### *Collection of conditioned medium (CM)*

CM were collected from SVPs (SVP-CM) or MSCs (MSC-CM) transfected with either anti-miR-132 or scrambled oligonucleotide after normoxia or H/S for 48h. Forty-eight hours later, medium was replaced with fresh one deprived of growth factors and the cells were cultured under normoxia or hypoxia. At the end of another 48h, CM was collected and concentrated (50X, Amicon ultra, Millipore). By this method we confirmed the higher yield of miR-132 in the CM.<sup>15</sup>

### *Experiments with CM*

HUVECs, adult rat cardiomyocytes or fibroblasts were cultured in 96-well plate (caspase-3/7 activity, BrdU proliferation assay), 6-well plates (expressional analyses) or 8-well chamber slides (immunocytochemistry). For HUVECs and fibroblasts, after 24h, medium were replaced with SVP- or MSC-CM collected after different treatments to SVP. Thirty-six hours later, cells were used for different assays. For cardiomyocytes, after 4h of plating in the laminin coated culture plates to allow the cells to settle down, medium was replaced with SVP-CM and cells were exposed to hypoxia for 12h, to mimic in vivo ischemia situation to the cardiomyocytes. After 12h, cells were used for caspase-3/7 activity measurement. In addition experiments were also performed to evaluate the ability of network formation by HUVECs after treatment with SVP- or MSC-CM (*vide infra*).

### *BrdU incorporation assay*

To study the effect of hypoxia on SVP proliferation, we used the BrdU incorporation assay. Following starvation, BrdU (10 $\mu$ mol/L) was added to the medium before cells were exposed to hypoxia. BrdU incorporation by SVPs was measured using a BrdU immunofluorescence assay kit from Roche, according to the manufacturer's instructions. Briefly, SVPs were fixed and made permeable with FixDenat solution for 20min, then incubated with monoclonal anti-BrdU peroxidase-conjugated antibody (anti-BrdU-POD) for 90min. Bound anti-BrdU-POD was detected by a substrate reaction, then quantified by an ELISA plate reader. Each experiment was performed in triplicate and repeated 5 times. Similar experiments were performed with SVP-CM.<sup>4, 16</sup>

### *Migration assays*

Mononuclear cells (MNC) were prepared from the peripheral blood collected from healthy volunteers. 5X10<sup>6</sup> MNC were placed in the upper chamber of 3  $\mu$ m pore-size filter-equipped transwell chambers (Corning) and allowed to migrate toward conditional or unconditional medium collected from SVPs subjected to hypoxia/starvation. The assays were stopped after 18h at 37°C, and cells that had invaded the membrane and migrated through the filter were fixed on the lower side of the filter and mounted with Vectashield containing DAPI. Five random fields were counted at 20X magnification for each chamber. Cells were then stained for antibodies against CD14 (FITC conjugated) and CD16 (APC conjugated, both from Invitrogen, UK) and the enrichment of CD14<sup>+</sup>CD16<sup>+</sup> cells among the migrated cells were assessed by flowcytometry (Canto II, BD Biosciences, UK).

### *In vitro matrigel assay*

SVPs pre-treated with anti-miR-132 or scrambled sequence and serum starved mixed with human umbilical vein endothelial cells (HUVEC, 1:4 ratio of SVPs to HUVEC respectively) were seeded in 8-well chamber slides at 25000 cells/well on top of 250 $\mu$ l gelified Matrigel (BD Biosciences, UK) and exposed to normal or 1% O<sub>2</sub> for 18h. At the end of experiment, floating cells were removed by washing and the endothelial networks were fixed with 2% PFA. Number of branches and total length of the networks were calculated using the Image-Pro Plus software on images taken at 40X magnification. Each condition was run in quadruplicates and assay was repeated three times. Similar experiments were performed with SVP-CM.

**Statistical Analysis**

Results are expressed as mean  $\pm$  standard error. Difference between multiple groups was analyzed using one-way ANOVA and difference between two groups using t-test (paired or unpaired as appropriate). For myocardial BF and expressional studies, when normality test failed, differences between groups were analyzed using Siegel-Tukey test. A P value of  $<0.05$  was considered statistically significant.



## References

1. Campagnolo P, Cesselli D, Al Haj Zen A, Beltrami AP, Krankel N, Katare R, Angelini G, Emanuelli C, Madeddu P. Human adult vena saphena contains perivascular progenitor cells endowed with clonogenic and proangiogenic potential. *Circulation*.121(15):1735-1745.
2. Katare R, Caporali A, Zentilin L, Avolio E, Sala-Newby G, Oikawa A, Cesselli D, Beltrami AP, Giacca M, Emanuelli C, Madeddu P. Intravenous Gene Therapy With PIM-1 Via a Cardiotropic Viral Vector Halts the Progression of Diabetic Cardiomyopathy Through Promotion of Prosurvival Signaling. *Circulation research*. 2011;108(10):1238-1251.
3. Jeppesen PL, Christensen GL, Schneider M, Nossent AY, Jensen HB, Andersen DC, Eskildsen T, Gammeltoft S, Hansen JL, Sheikh SP. Angiotensin II type 1 receptor signalling regulates microRNA differentially in cardiac fibroblasts and myocytes. *British journal of pharmacology*. 2011.
4. Katare R, Caporali A, Emanuelli C, Madeddu P. Benfotiamine improves functional recovery of the infarcted heart via activation of pro-survival G6PD/Akt signaling pathway and modulation of neurohormonal response. *Journal of molecular and cellular cardiology*.49(4):625-638.
5. Meloni M, Caporali A, Graiani G, Lagrasta C, Katare R, Van Linthout S, Spillmann F, Campesi I, Madeddu P, Quaini F, Emanuelli C. Nerve growth factor promotes cardiac repair following myocardial infarction. *Circulation research*.106(7):1275-1284.
6. de Simone G, Wallerson DC, Volpe M, Devereux RB. Echocardiographic measurement of left ventricular mass and volume in normotensive and hypertensive rats. Necropsy validation. *Am J Hypertens*. 1990;3(9):688-696.
7. Katare RG, Caporali A, Oikawa A, Meloni M, Emanuelli C, Madeddu P. Vitamin B1 analog benfotiamine prevents diabetes-induced diastolic dysfunction and heart failure through Akt/Pim-1-mediated survival pathway. *Circ Heart Fail*.3(2):294-305.
8. Spillmann F, Graiani G, Van Linthout S, Meloni M, Campesi I, Lagrasta C, Westermann D, Tschope C, Quaini F, Emanuelli C, Madeddu P. Regional and global protective effects of tissue kallikrein gene delivery to the peri-infarct myocardium. *Regenerative medicine*. 2006;1(2):235-254.
9. Krankel N, Katare RG, Siragusa M, Barcelos LS, Campagnolo P, Mangialardi G, Fortunato O, Spinetti G, Tran N, Zacharowski K, Wojakowski W, Mroz I, Herman A, Manning Fox JE, MacDonald PE, Schanstra JP, Bascands JL, Ascione R, Angelini G, Emanuelli C, Madeddu P. Role of kinin B2 receptor signaling in the recruitment of circulating progenitor cells with neovascularization potential. *Circulation research*. 2008;103(11):1335-1343.
10. Swedberg K, Eneroth P, Kjekshus J, Wilhelmsen L. Hormones regulating cardiovascular function in patients with severe congestive heart failure and their relation to mortality. CONSENSUS Trial Study Group. *Circulation*. 1990;82(5):1730-1736.
11. Stone OA, Richer C, Emanuelli C, van Weel V, Quax PH, Katare R, Kraenkel N, Campagnolo P, Barcelos LS, Siragusa M, Sala-Newby GB, Baldessari D, Mione M, Vincent MP, Benest AV, Al Haj Zen A, Gonzalez J, Bates DO, Alhenc-Gelas F, Madeddu P. Critical role of tissue kallikrein in vessel formation and maturation: implications for therapeutic revascularization. *Arteriosclerosis, thrombosis, and vascular biology*. 2009;29(5):657-664.
12. Siragusa M, Katare R, Meloni M, Damilano F, Hirsch E, Emanuelli C, Madeddu P. Involvement of phosphoinositide 3-kinase gamma in angiogenesis and healing of experimental myocardial infarction in mice. *Circulation research*.106(4):757-768.

13. Bonewald LF, Harris SE, Rosser J, Dallas MR, Dallas SL, Camacho NP, Boyan B, Boskey A. von Kossa staining alone is not sufficient to confirm that mineralization in vitro represents bone formation. *Calcified tissue international*. 2003;72(5):537-547.
14. Caporali A, Meloni M, Vollenkle C, Bonci D, Sala-Newby GB, Addis R, Spinetti G, Losa S, Masson R, Baker AH, Agami R, le Sage C, Condorelli G, Madeddu P, Martelli F, Emanuelli C. Deregulation of microRNA-503 contributes to diabetes mellitus-induced impairment of endothelial function and reparative angiogenesis after limb ischemia. *Circulation*. 2011;123(3):282-291.
15. Chen TS, Lai RC, Lee MM, Choo AB, Lee CN, Lim SK. Mesenchymal stem cell secretes microparticles enriched in pre-microRNAs. *Nucleic acids research*. 2010;38(1):215-224.
16. Caporali A, Pani E, Horrevoets AJ, Kraenkel N, Oikawa A, Sala-Newby GB, Meloni M, Cristofaro B, Graiani G, Leroyer AS, Boulanger CM, Spinetti G, Yoon SO, Madeddu P, Emanuelli C. Neurotrophin p75 receptor (p75NTR) promotes endothelial cell apoptosis and inhibits angiogenesis: implications for diabetes-induced impaired neovascularization in ischemic limb muscles. *Circulation research*. 2008;103(2):e15-26.

## Supplemental Figure Legends

### Online Table I

Echocardiographic parameters in CD1-FOXO<sup>nu/nu</sup> immunodeficient mice injected with SVPs (1x10<sup>6</sup>) or vehicle. Vehicle – vehicle treated; SVP – SVP treated. LVAWs, LV anterior wall, end-systole; LVAWd, LV anterior wall, end-diastole; LVPWs, LV posterior wall, end-systole; LVPWd, LV posterior wall, end-diastole; LVESV, LV end-systolic volume; LVEDV, LV end-diastolic volume; LVSV, LV stroke volume; LVEF, LV ejection fraction; LVFS, LV fractional shortening; HR, heart rate; CO, cardiac output; LVEDP, LV end diastolic pressure. LV pressure measurements were performed prior to sacrifice. Data are presented as means±SE (n=6 mice per group). \*P<0.05 vs. vehicle-treated post-MI.

### Online Figure I

**A&B.** Characterization of antigenic profile of SVPs by flow cytometry (**A**) and immunocytochemistry (**B**). **C.** Representative confocal images showing the acquisition of cardiac specific markers by SVPs in selective culture conditions. **D&E.** Characterization of SVP immunogenic profile by flow cytometry (**D**) and semi-quantitative RT-PCR (**E**). Scale bars are 50µm; α-SA - alpha sarcomeric actin. n.d - non detectable; Data are means±SE. Each experiment was repeated three times.

### Online Figure II

SVP transplantation attenuates early LV dysfunction in immunocompetent mice. Bar graphs showing pre-MI and post-MI values: (**A**) LV anterior wall systole (LVAWs), (**B**) LV anterior wall diastole (LVAWd), (**C**) LV end-systolic volume (LVESV), (**D**) LV end-diastolic volume (LVEDV), (**E**) LV stroke volume (LVSV), (**F**) LV ejection fraction (LVEF), (**G**) LV fractional shortening (LVFS), (**H**) cardiac output (CO), (**I**) LV end systolic pressure (LVESP), (**J**) LV end diastolic pressure (LVEDP) and (**K**) dP/dt. (**L**) Representative pressure/volume loops. Cells were injected at the time of MI induction. Data are presented as means±SE (n= 11 mice per group). \*\*P<0.01 vs. vehicle-treated post-MI.

### Online Figure III

**A.** Kaplan Meier survival curve. **B&C.** Bar graphs showing echocardiographic parameters. Data are means±SE (n=13 mice per group). \*\*P<0.01 vs. vehicle-treated; §§P<0.01 vs. corresponding-treatment group at 14d post-MI; †P<0.05 vs. SVP-transplanted. **D.** Bar graphs showing markers of neurohormonal activation. **E.** Representative western blots and bar graphs showing the level of angiotensin II type 1 receptor (AT1R) expression in myocardium. Data are means±SE. (n=6 mice per group). ##P<0.01 vs. sham; \*P<0.05 and \*\*P<0.01 vs. vehicle at corresponding time-point.

### Online Figure IV

Representative images and bar graph showing EC proliferation (**A**, arrow points PCNA positive cells) and apoptosis (**B**, arrow points TUNEL positive cells) in the peri-infarct zone, assessed by PCNA and TUNEL staining, respectively. Dotted lines delineate the infarct zone. Scale bars are 50µm. Data are means±SE (n=6 mice per group). \*P<0.05 and \*\*P<0.01 vs. vehicle.

### Online Figure V

Effect of MSC transplantation on LV angiogenesis, remodeling, apoptosis. Bar graphs showing the capillary (**A**) and arteriole density (**B**), scar dimension (**C**) and cardiomyocyte apoptosis in the border zone (**D**) and interstitial fibrosis in the remote zone at 42d post-MI. Data are means±SE (n=4 mice per group). \*P<0.05 and \*\*P<0.01 vs. vehicle.

### Online Figure VI

Bar graphs showing the levels of GFs in SVP-CM under normoxia (normoxic-CM) or hypoxia/serum starvation (H/S-CM); unconditioned medium (UCM); \*P<0.05 vs. normoxic-CM.

### Online Figure VII

Representative images showing the expression of VEGF-B in Mac-3 (1) and CD45 positive cells (2) in hearts harvested at 5d post-MI and bar graph showing the average VEGF-B expression in CD45 positive and negative cells, expressed as fluorescence intensity. \*\*\*P<0.001 vs. vehicle. Scale bars are 50µm.

### Online Figure VIII

**A.** Bar graphs showing the effect of anti-miR-132 or scrambled sequence (Scr) transfection on SVP proliferation (BrdU incorporation) and apoptosis (Caspase 3/7 activity) under normoxia or hypoxia/serum starvation (H/S). Vehicle of transfection (V). Data are means±SE from experiments performed in quadruplicates. \*P<0.05, \*\*P<0.01 and \*\*\*P<0.001 vs. corresponding group under normoxia; §§P<0.01 vs. vehicle and ###P<0.01 vs. Scr under corresponding culture conditions. **B.** Representative images (i to iv) and bar graphs (v) showing the attenuation of the SVP ability to enhance network formation by HUVECs. SVPs were pre-treated with anti-miR-132, scrambled sequence (Scr) or vehicle and co-cultured with human umbilical vein endothelial cells (HUVEC) in 1:4 ratio respectively on matrigel. Values are expressed as cumulative tube length per field and are means±SE. ####P<0.001 vs. HUVECs alone and §§P<0.01 vs. scrambled sequence. Experiments are performed in quadruplicates and repeated three times. Scale bars are 100µm.

### Online Figure IX

Bar graphs showing BrdU incorporation (**A**) and representative western blots and bar graphs showing Akt phosphorylation (**B**) in HUVECs treated with SVP-CM. Data (means±SE) are represented as fold changes to UCM from experiments performed in quadruplicates. φP<0.01 vs. UCM; §P<0.05 and §§P<0.01 vs. corresponding group under normoxic SVP-CM; ##P<0.01 and ####P<0.001 vs. Scr.

### Online Figure X

**A.** Bar graphs showing the level of angiogenic growth factors and miR-132 in SVP- and MSC-CM. Unconditioned medium (UCM) for SVPs is EBM-2 with 2% FBS and UCM for MSCs is mesenchymal stem cell media with 2% FBS and without growth factors. Data are means±SE. miR-132 levels are expressed as fold change vs. normoxic SVP-CM. \*\*P<0.01 vs. UCM; §P<0.05 and §§P<0.01 vs. normoxic CM; ###P<0.01 vs. SVP-CM under the same culture conditions. **B.** Representative images (i-vi) and bar graphs (vii) showing the network formation by HUVEC after treatment with UCM (i&iv) and SVP- (ii&iii) or MSC-CM (v&vi). Values are expressed as cumulative tube length per field and are means±SE. Experiments were performed in quadruplicates and repeated three times. Scale bars are 100µm. \*\*P<0.01 vs. UCM; ####P<0.001 vs. SVP-CM under the same culture conditions.

### Online Figure XI

**A.** Representative confocal images showing the localization of p120RasGAP in endothelial cells (ii), cardiomyocytes (iii) and fibroblasts (iv) in the myocardium at 14d post-MI. Negative control (i) without primary antibody to p120RasGAP was used as reference. Scale bars are 50µm. **B.** Representative western blots and bar graph showing the levels of miR-132 target gene p120RasGAP in myocardium. **C.** Bar graphs showing hemodynamic data (i&ii), EC apoptosis (iii) and proliferation (iv) at 14d post-MI. Data are means±SE (n=5 mice per group except for hemodynamic measurements which consisted of 6 mice). ##P<0.01 and ###P<0.001 vs. sham; \*P<0.01 and \*\*\*P<0.001 vs. vehicle; °P<0.05 and °°P<0.01 vs. non-transfected SVPs; φP<0.05 and φφP<0.01 vs. Scr-transfected SVPs.

### **Online Figure XII**

Bar graphs showing long-term inhibition of miR-132 expression in SVPs transfected with anti-miR-132. Experiments were performed in triplicates. Data are means±SE; \*\*\*P<0.001 vs. scrambled sequence.

### **Online Figure XIII**

Bar graph showing the number of Dil-positive SVPs in the myocardium at 14d post-MI. Data expressed as number of Dil-positive cells per million cell nuclei and represented as means±SE (n=6 mice per group).

### **Online Figure XIV**

Bar graph showing caspase-3/7 activity in adult rat cardiomyocytes exposed to hypoxia after treatment with SVP-CM. Data are means±SE from experiment performed in quadruplicate. ##P<0.01 vs. unconditioned medium (UCM).

### **Online Figure XV**

**A.** Representative images showing different cardiac stem cell populations such as (i) primitive cells (c-Kit(+) GATA4(-)α-sarcomeric actin(-)), (ii) progenitors ((c-Kit(+)GATA4(+)α-sarcomeric actin(-)), (iii) precursors (c-Kit(+) GATA4(+)α-sarcomeric actin(+)), (iv) proliferating c-Kit cells (c-Kit(+)Mcm5(+) α-sarcomeric actin(-)) and (v) mastocytes (c-kit(+)Mast cell tryptase (+) GATA4(-)α-sarcomeric actin(-)) in the infarcted myocardium at 14 days post-MI. Resident stem cells are identified as the c-Kit positive cells negative for mast cell tryptase. Scale bars are 15µm except for (ii) which is 50µm. **B.** Bar graphs showing the quantification of different populations of cardiac stem cells at 14d post-MI. Data are means±SE (n= 7 in vehicle and 9 in SVP treated group). \*P<0.05 vs. vehicle.

**Online Figure XVI.** Representative images showing Angiotenin-II differentiated myofibroblasts staining positive for α-smooth muscle actin and MeCP2. Scale bars are 50µm.

**Online Figure XVII.** Representative microscopic images of Von Kossa staining in the infarct zone of the myocardium at 42d post-MI. Fibula of 3 weeks old mice was used as positive control. Two representative images are shown from each group. Scale bars are 100µm.

## **Legend for Online Videos**

### **Online video I**

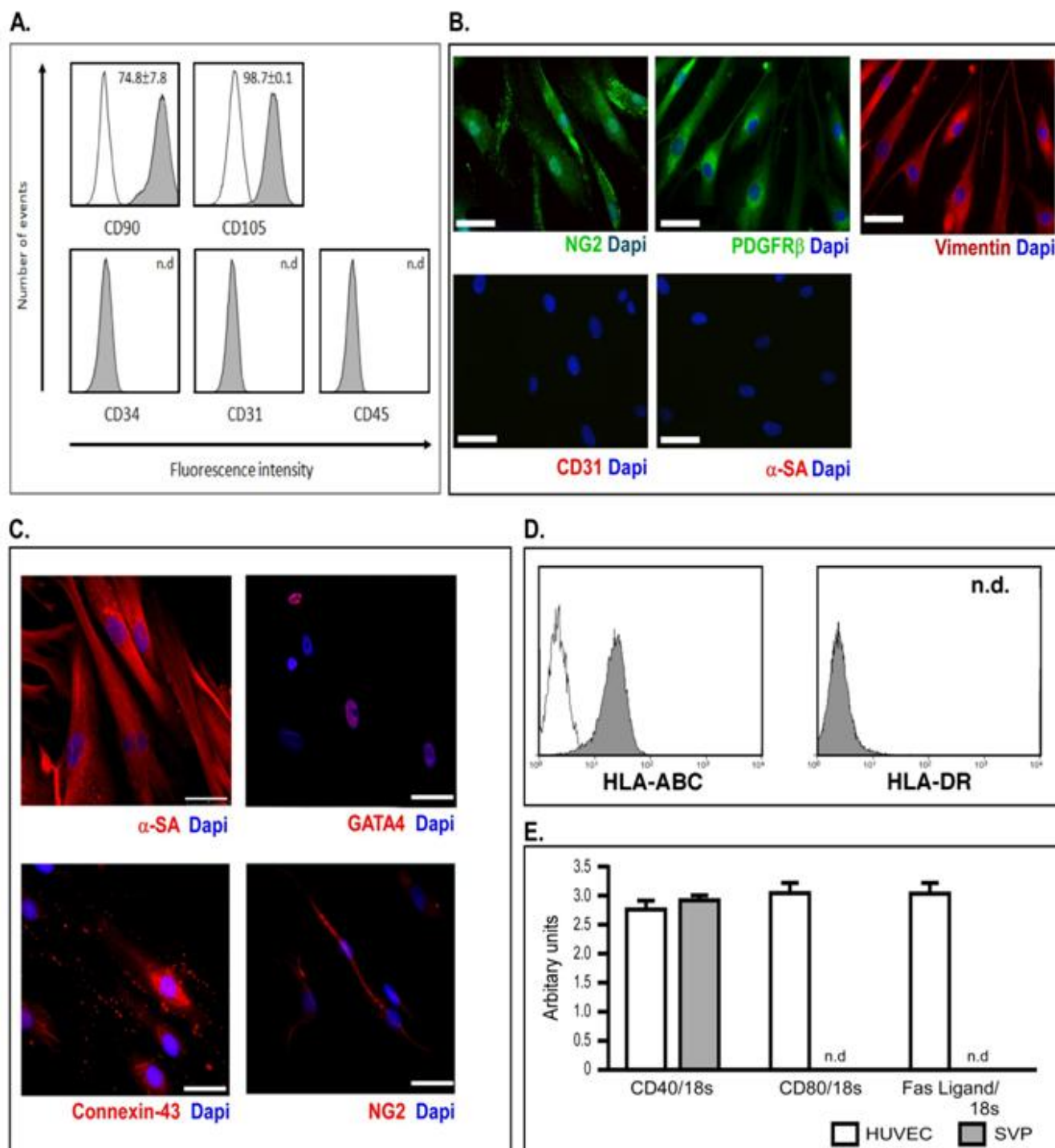
Serial z-stack images of myocardium showing the alignment of transplanted Dil-labelled SVPs (stained in red) along the perfused vessels, which were identified by staining with intracardially-injected Isolectin (green). Nuclei are identified with Dapi.



	Pre-MI		Post-MI	
	Vehicle	SVP	Vehicle	SVP
LVAWs (mm)	1.27±0.02	1.26±0.03	0.33±0.02	0.49±0.02*
LVAWd (mm)	0.99±0.03	0.91±0.05	0.27±0.02	0.39±0.02*
LVPWs (mm)	1.21±0.05	1.24±0.06	1.27±0.08	1.37±0.07
LVPWd (mm)	0.97±0.05	1.01±0.04	1.08±0.04	1.06±0.06
LVESD (mm)	2.22±0.15	2.24±0.13	4.68±0.15	4.35±0.18
LVEDD (mm)	3.61±0.16	3.70±0.08	5.16±0.12	4.95±0.17
LVESV (μl)	12.9±0.7	14.9±2.4	108.6±8.3	86.3±8.8
LVEDV (μl)	53.4±1.5	56.7±2.9	132.1±7.7	116.4±9.5
LVSV (μl)	40.4±1.7	40.6±3.7	23.5±2.4	30.1±3.5*
LVEF (%)	75.6±1.6	73.7±2.9	18.2±2.2	26.2±1.74*
LVFS (%)	38.6±1.8	39.4±0.9	11.8±1.9	11.7±0.4
HR (b/min)	455±14	447±5	534±9	541±9
CO (ml/min)	18.4±2.1	17.9±1.7	12.5±1.2	16.3±0.8*
LVEDP (mmHg)	-	-	10.0±0.7	7.8±0.5*
dP/dt <sub>max</sub> (mmHg/Sec)	-	-	4370±154	4881±73*
dP/dt <sub>min</sub> (mmHg/Sec)	-	-	-3434±121	-3935±138*

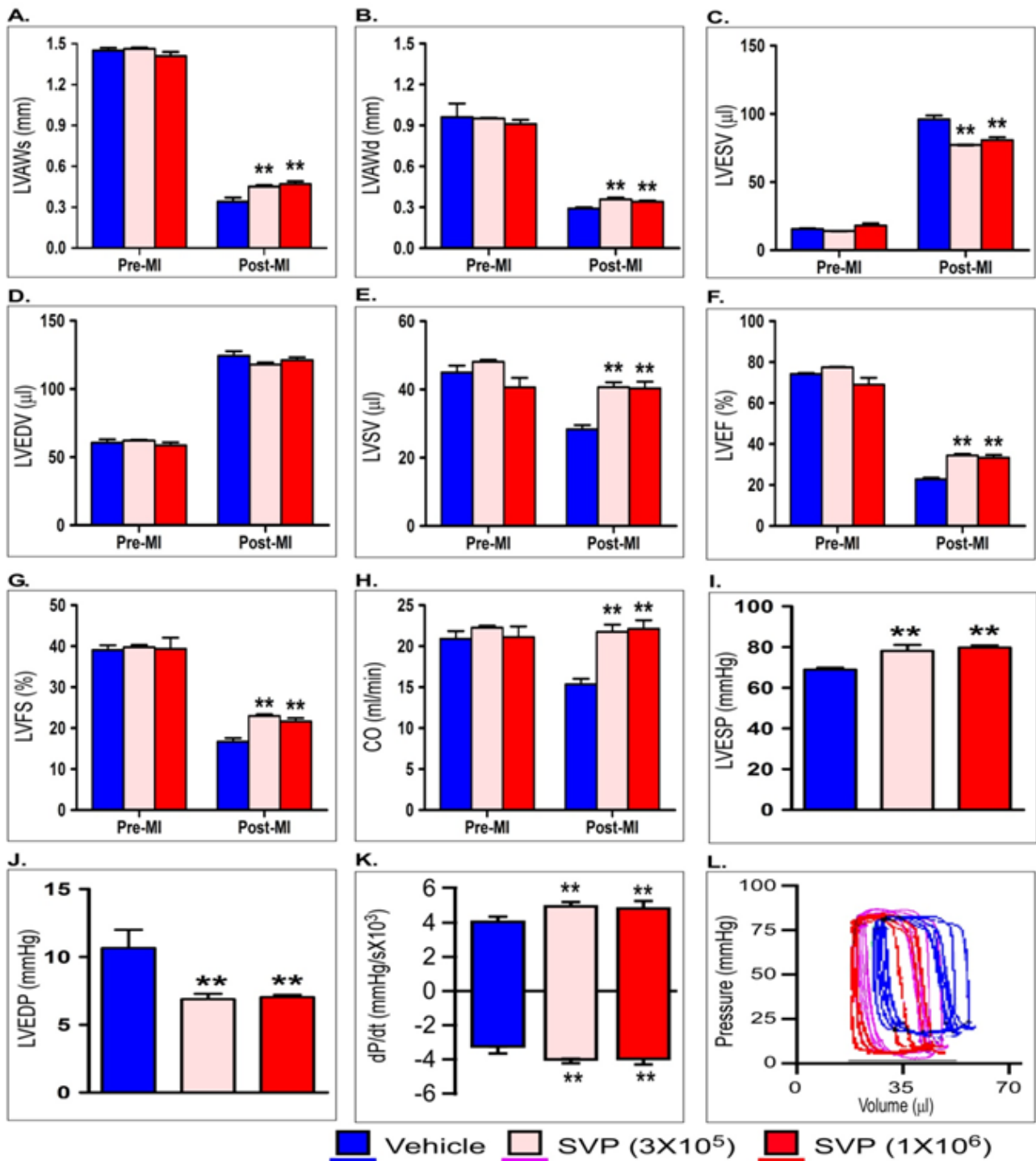
#### Online Table 1

Echocardiographic parameters in CD1-FOXO<sup>nu/nu</sup> immunodeficient mice injected with SVPs (1×10<sup>6</sup>) or vehicle. Vehicle – vehicle treated; SVP – SVP treated. LVAWs, LV anterior wall, end-systole; LVAWd, LV anterior wall, end-diastole; LVPWs, LV posterior wall, end-systole; LVPWd, LV posterior wall, end-diastole; LVESV, LV end-systolic volume; LVEDV, LV end-diastolic volume; LVSV, LV stroke volume; LVEF, LV ejection fraction; LVFS, LV fractional shortening; HR, heart rate; CO, cardiac output; LVEDP, LV end diastolic pressure. LV pressure measurements were performed prior to sacrifice. Data are presented as means±SE (n=6 mice per group). \*P<0.05 vs. vehicle-treated post-MI.



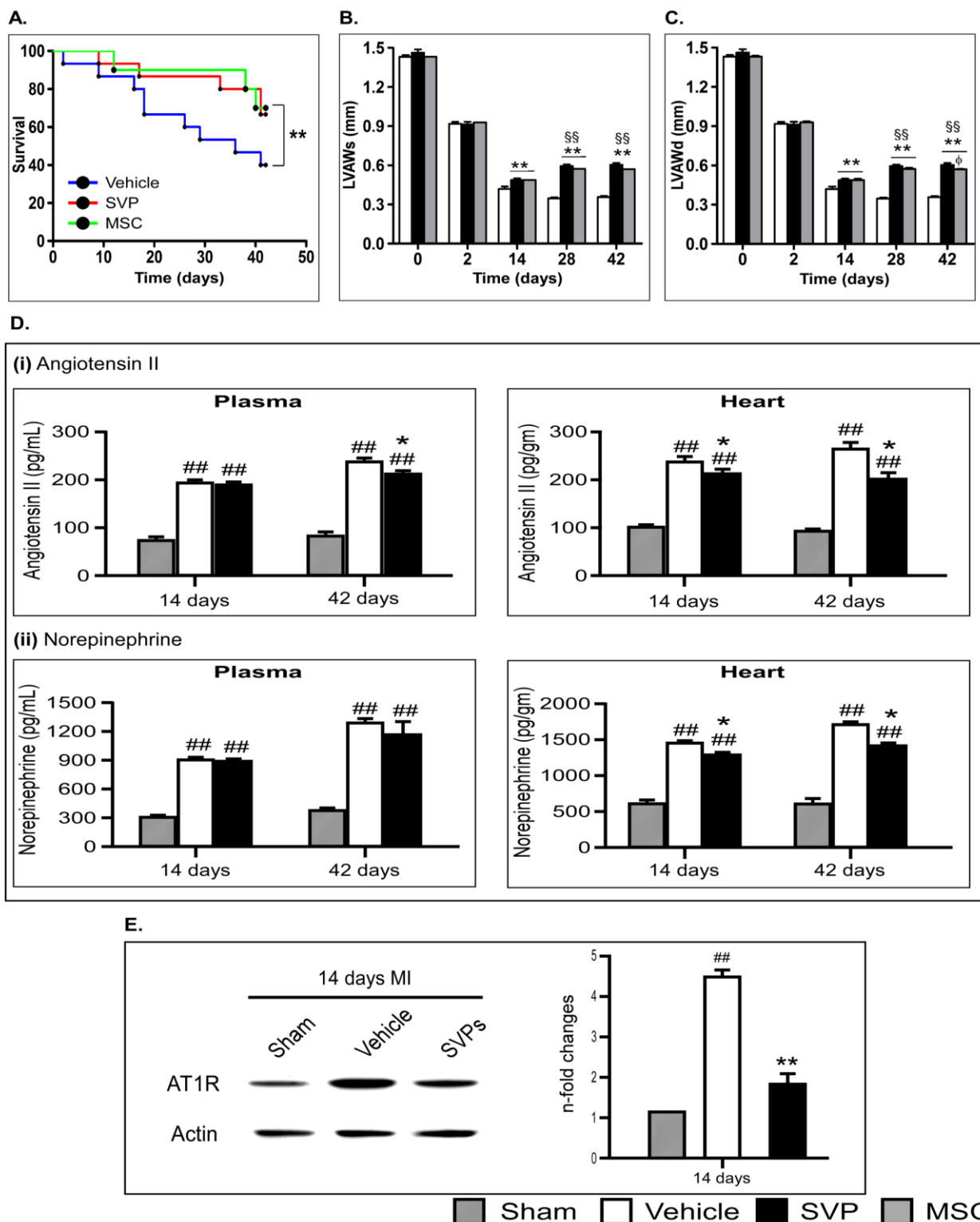
### Online Figure 1

**A&B.** Characterization of antigenic profile of SVPs by flow cytometry (**A**) and immunocytochemistry (**B**). **C.** Representative confocal images showing the acquisition of cardiac specific markers by SVPs in selective culture conditions. **D&E.** Characterization of SVP immunogenic profile by flow cytometry (**D**) and semi-quantitative RT-PCR (**E**). Scale bars are 50 $\mu$ m;  $\alpha$ -SA - alpha sarcomeric actin. n.d - non detectable; Data are means $\pm$ SE. Each experiment was repeated three times.



### Online Figure II

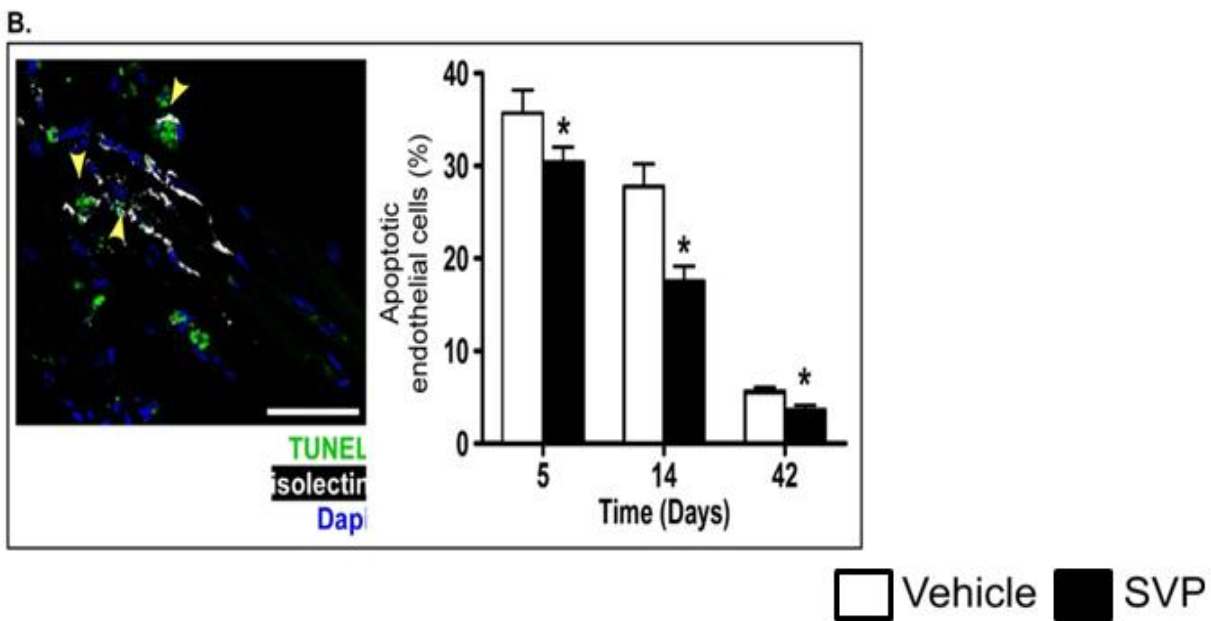
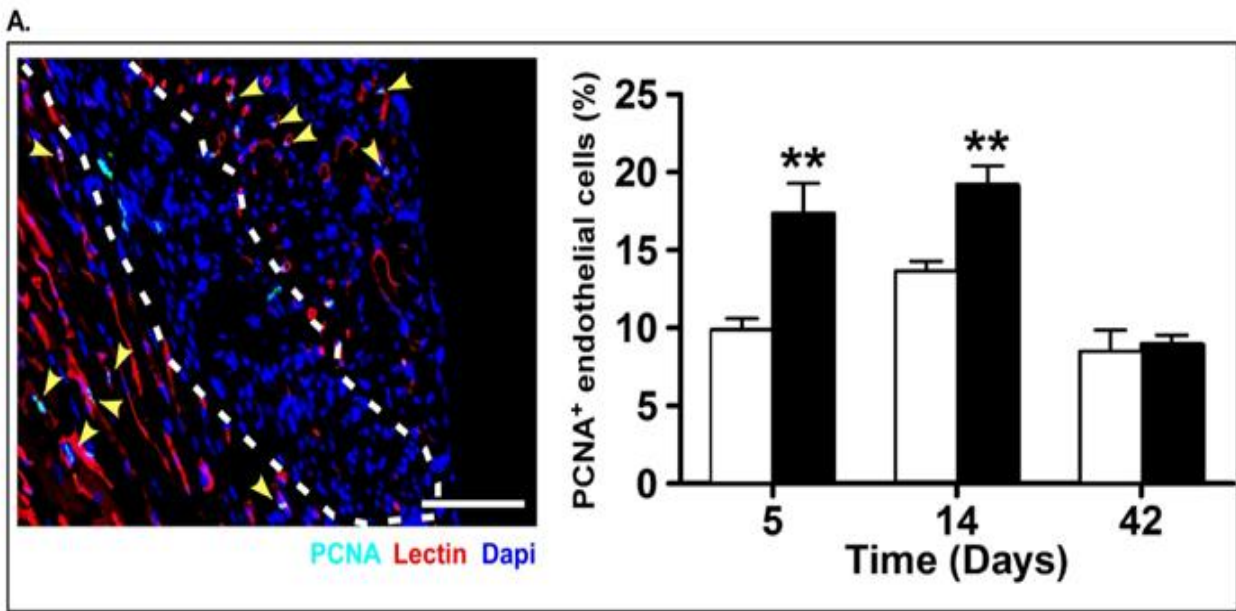
SVP transplantation attenuates early LV dysfunction in immunocompetent mice. Bar graphs showing pre-MI and post-MI values: (A) LV anterior wall systole (LVAVs), (B) LV anterior wall diastole (LVAVd), (C) LV end-systolic volume (LVESV), (D) LV end-diastolic volume (LVEDV), (E) LV stroke volume (LVS), (F) LV ejection fraction (LVEF), (G) LV fractional shortening (LVFS), (H) cardiac output (CO), (I) LV end systolic pressure (LVESP), (J) LV end diastolic pressure (LVEDP) and (K) dP/dt. (L) Representative pressure/volume loops. Cells were injected at the time of MI induction. Data are presented as means±SE (n= 11 mice per group). \*\*P<0.01 vs. vehicle-treated post-MI.



### Online Figure III

**A.** Kaplan Meier survival curve. **B&C.** Bar graphs showing echocardiographic parameters. Data are means±SE (n=13 mice per group). \*\*P<0.01 vs. vehicle-treated; §§P<0.01 vs. corresponding-treatment group at 14d post-MI; †P<0.05 vs. SVP-transplanted.

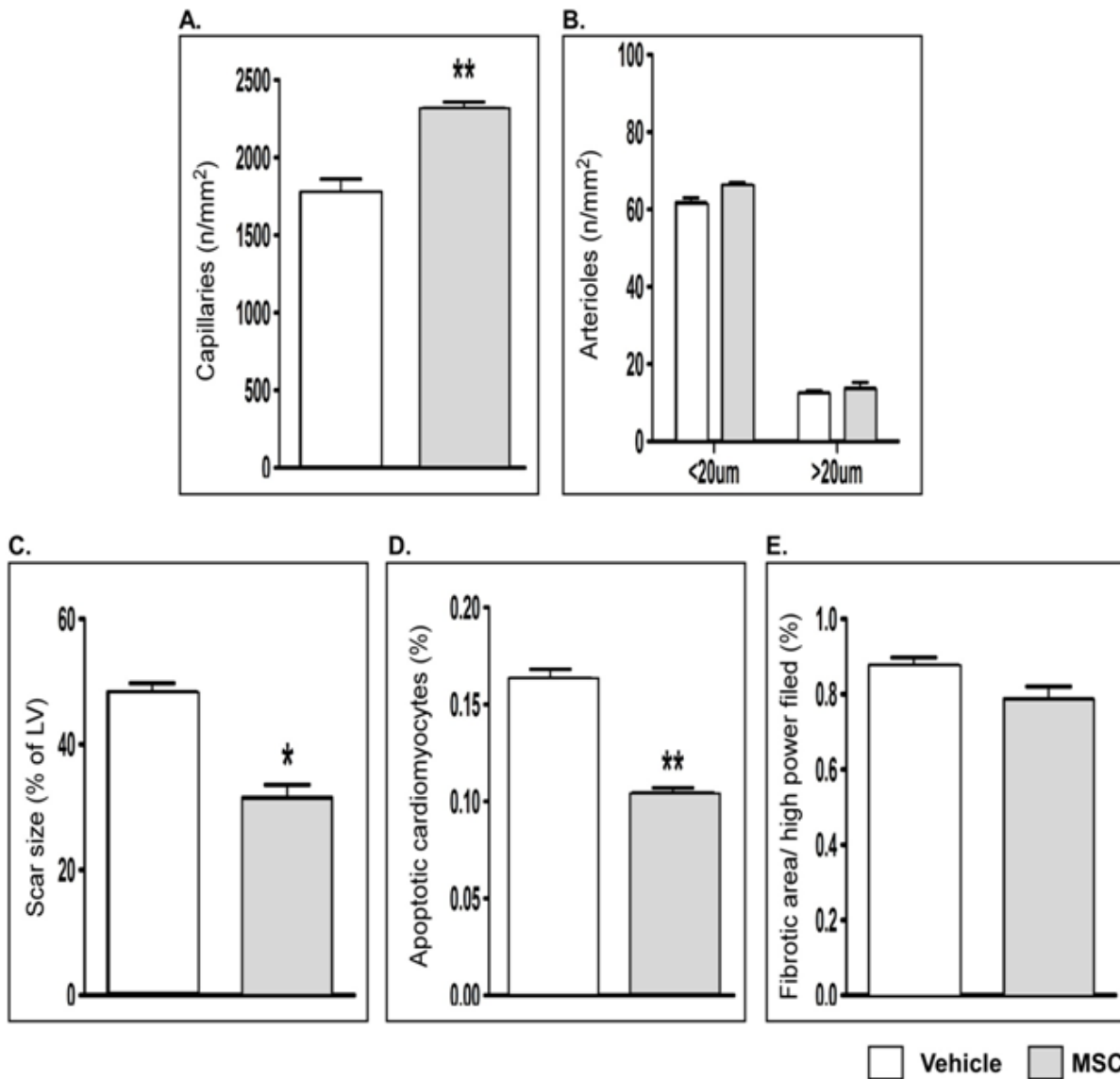
**D.** Bar graphs showing markers of neurohormonal activation. **E.** Representative western blots and bar graphs showing the level of angiotensin II type 1 receptor (AT1R) expression in myocardium. Data are means±SE. (n=6 mice per group). ##P<0.01 vs. sham; \*P<0.05 and \*\*P<0.01 vs. vehicle at corresponding time-point.



**Online Figure IV**

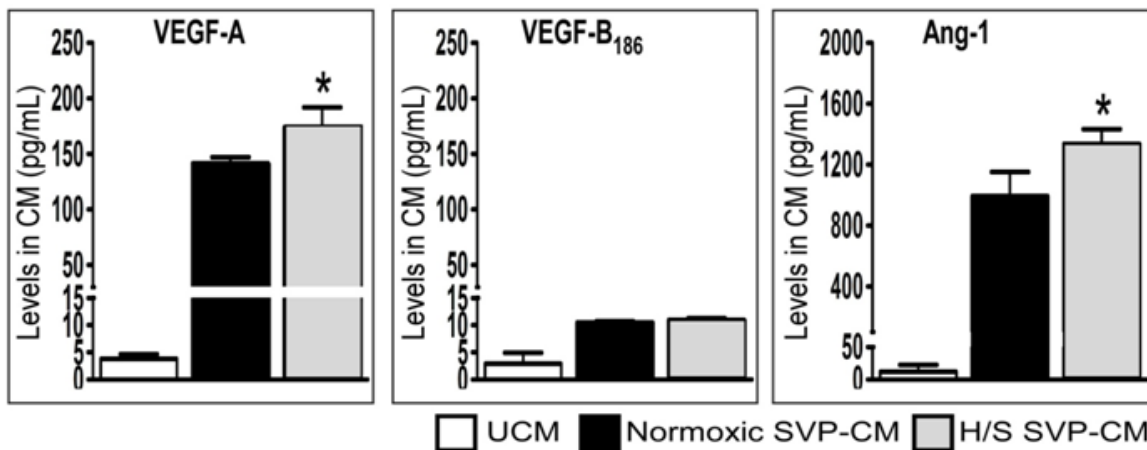
Representative images and bar graph showing EC proliferation (**A**, arrow points PCNA positive cells) and apoptosis (**B**, arrow points TUNEL positive cells) in the peri-infarct zone, assessed by PCNA and TUNEL staining, respectively. Dotted lines delineate the infarct zone. Scale bars are 50µm. Data are means±SE (n=6 mice per group). \*P<0.05 and \*\*P<0.01 vs. vehicle.





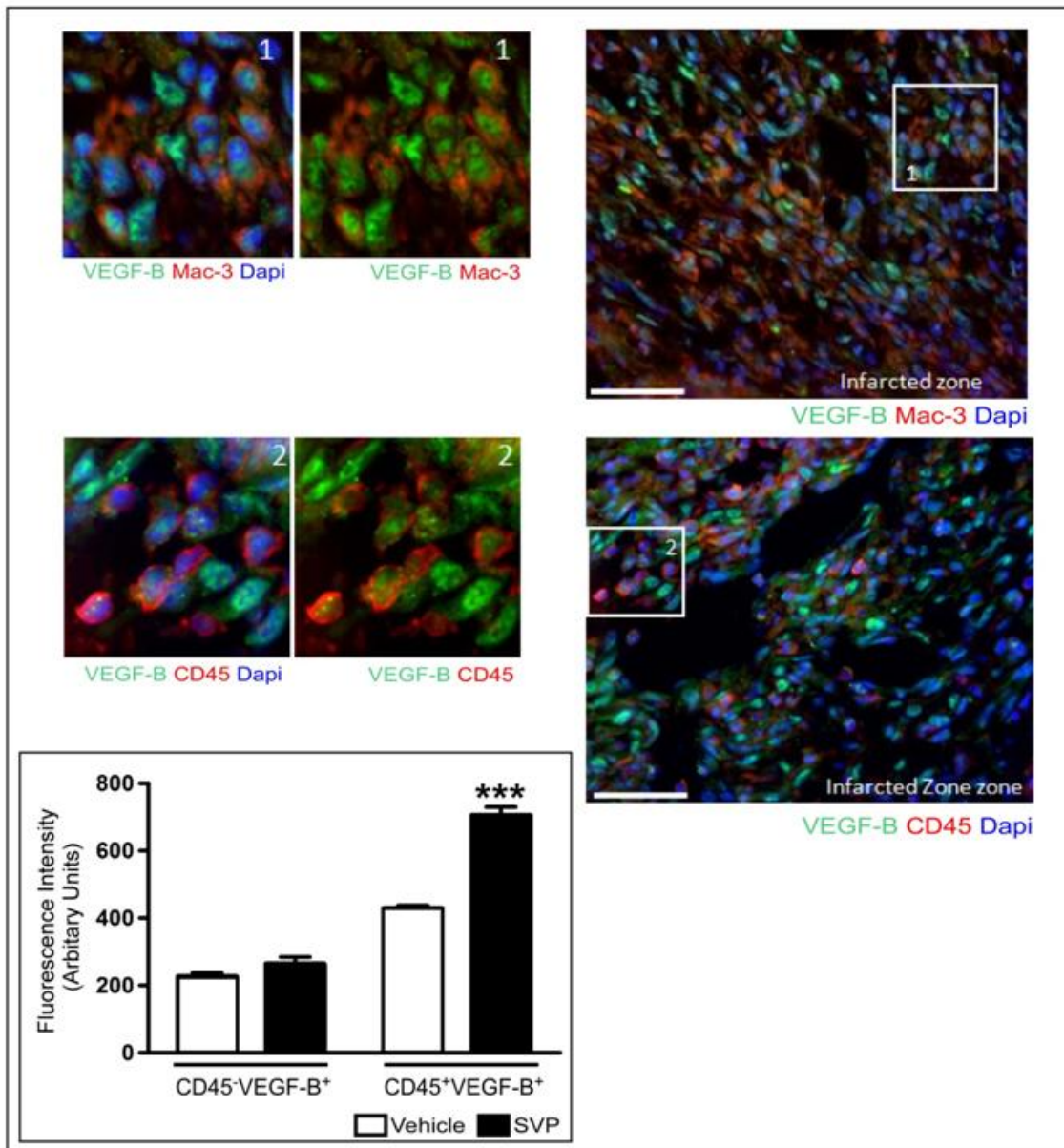
**Online Figure V**

Effect of MSC transplantation on LV angiogenesis, remodeling, apoptosis. Bar graphs showing the capillary (A) and arteriole density (B), scar dimension (C) and cardiomyocyte apoptosis in the border zone (D) and interstitial fibrosis in the remote zone at 42d post-MI. Data are means±SE (n=4 mice per group). \*P<0.05 and \*\*P<0.01 vs. vehicle.



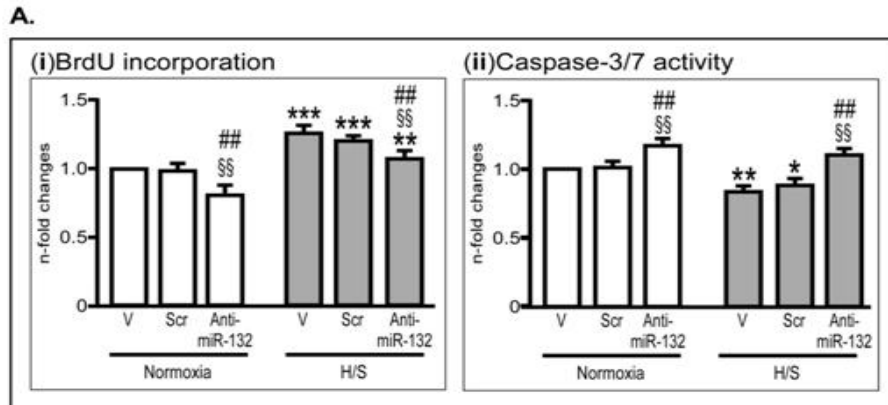
### Online Figure VI

Bar graphs showing the levels of GFs in SVP-CM under normoxia (normoxic-CM) or hypoxia/serum starvation (H/S-CM); unconditioned medium (UCM); \*P<0.05 vs. normoxic-CM.

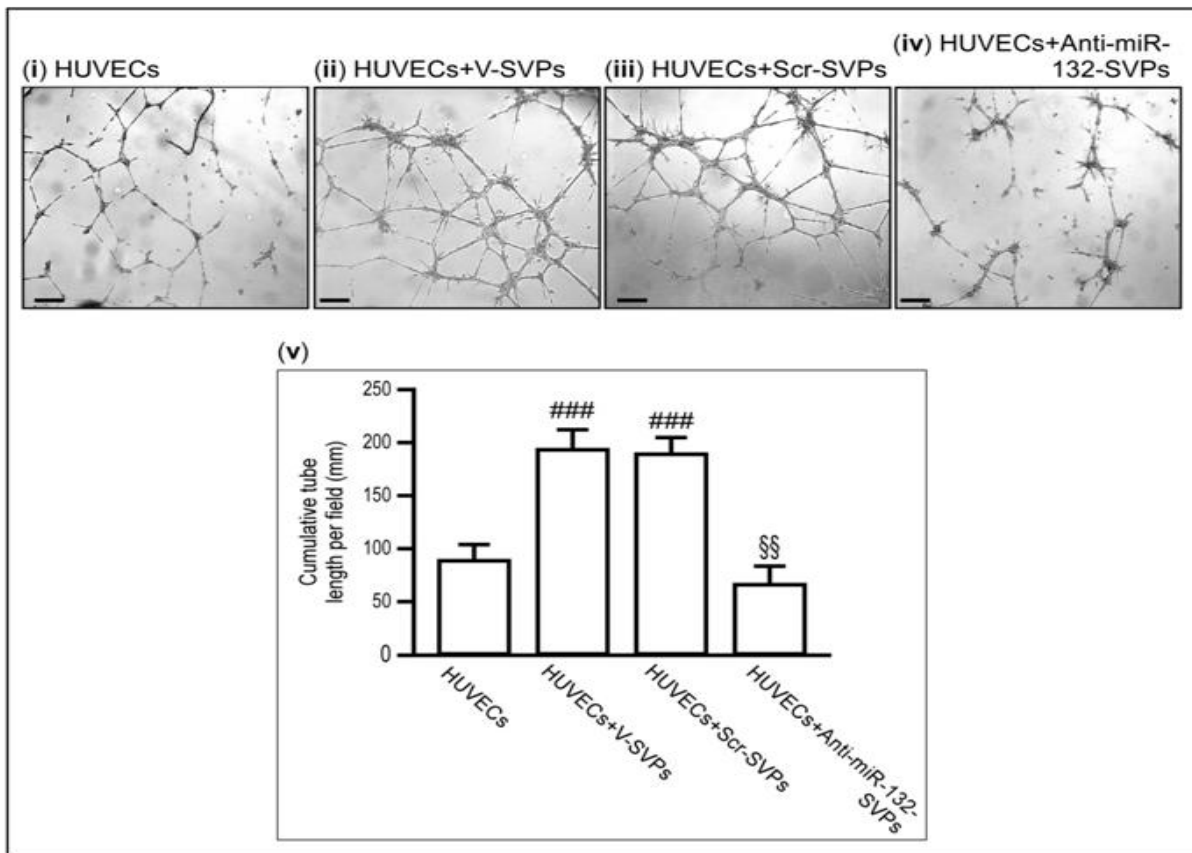


### Online Figure VII

Representative images showing the expression of VEGF-B in Mac-3 (1) and CD45 positive cells (2) in hearts harvested at 5d post-MI and bar graph showing the average VEGF-B expression in CD45 positive and negative cells, expressed as fluorescence intensity. \*\*\*P<0.001 vs. vehicle. Scale bars are 50µm.

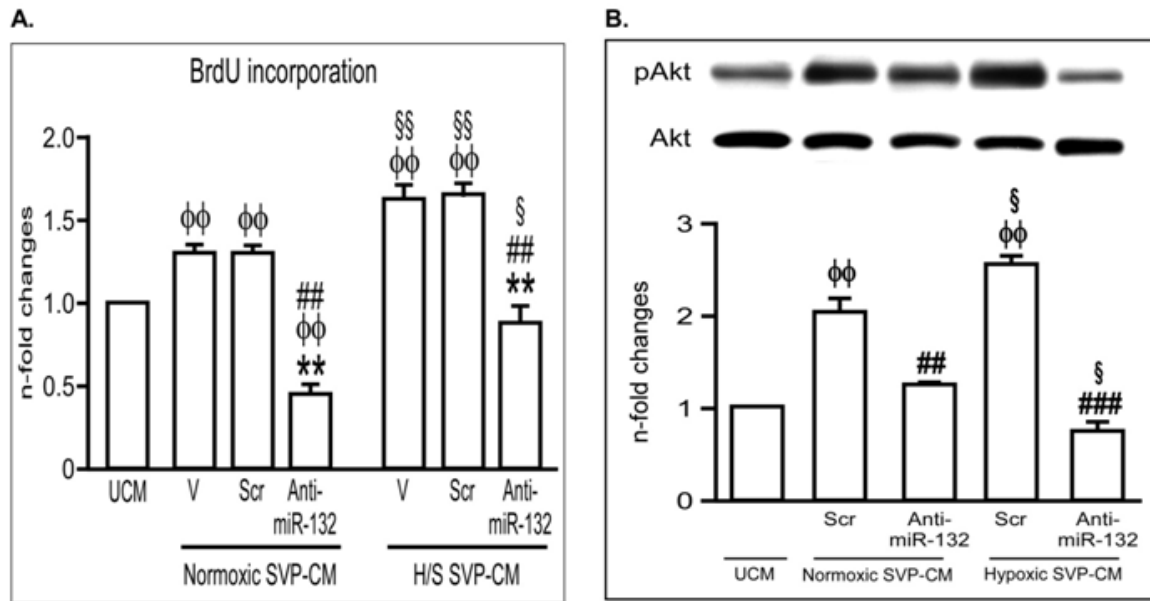


**B.**



### Online Figure VIII

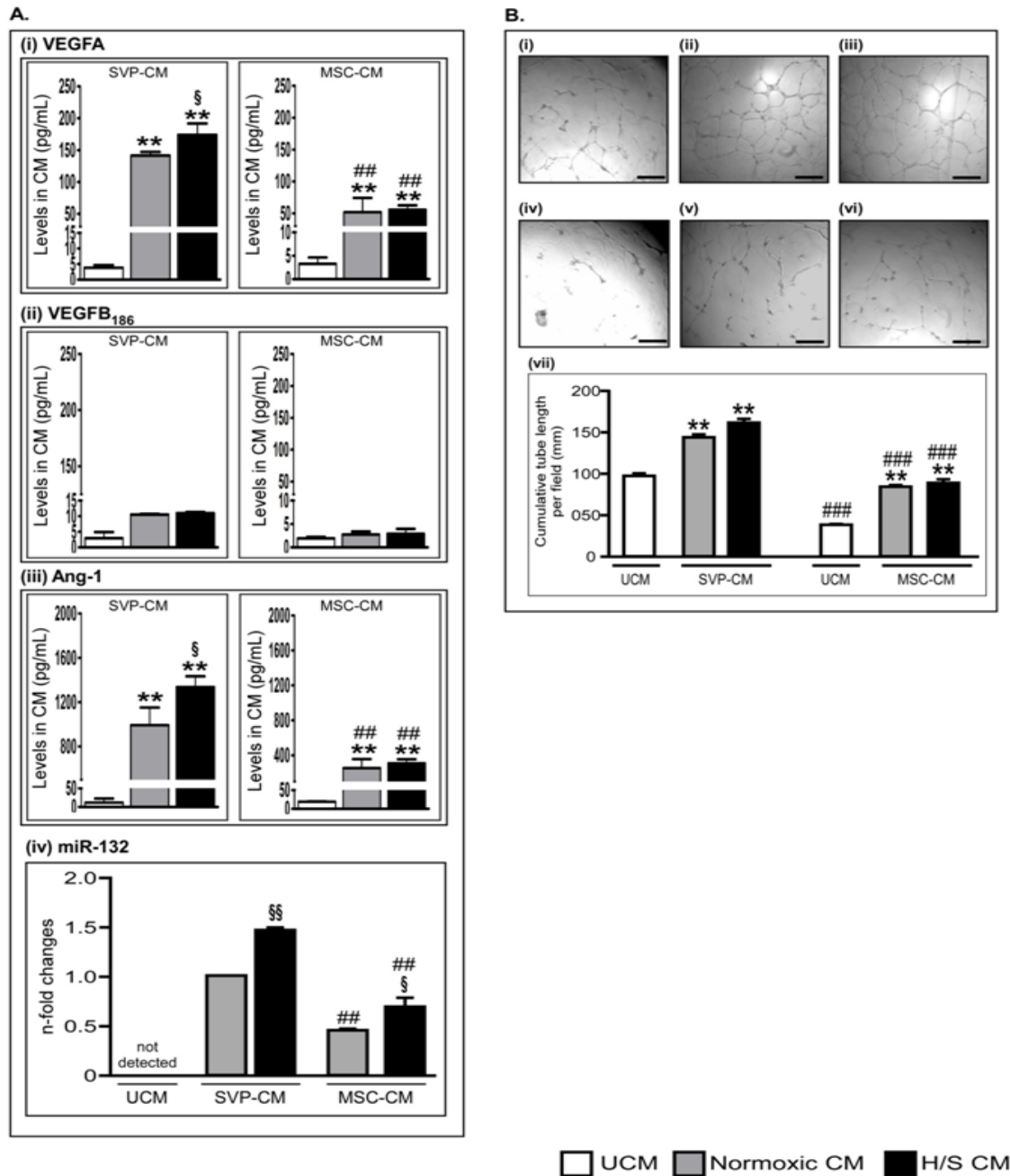
**A.** Bar graphs showing the effect of anti-miR-132 or scrambled sequence (Scr) transfection on SVP proliferation (BrdU incorporation) and apoptosis (Caspase 3/7 activity) under normoxia or hypoxia/serum starvation (H/S). Vehicle of transfection (V). Data are means±SE from experiments performed in quadruplicates. \*P<0.05, \*\*P<0.01 and \*\*\*P<0.001 vs. corresponding group under normoxia; §§P<0.01 vs. vehicle and ###P<0.01 vs. Scr under corresponding culture conditions. **B.** Representative images (i to iv) and bar graphs (v) showing the attenuation of the SVP ability to enhance network formation by HUVECs. SVPs were pre-treated with anti-miR-132, scrambled sequence (Scr) or vehicle and co-cultured with human umbilical vein endothelial cells (HUVEC) in 1:4 ratio respectively on matrigel. Values are expressed as cumulative tube length per field and are means±SE. ###P<0.001 vs. HUVECs alone and §§P<0.01 vs. scrambled sequence. Experiments are performed in quadruplicates and repeated three times. Scale bars are 100µm.



### Online Figure IX

Bar graphs showing BrdU incorporation (**A**) and representative western blots and bar graphs showing Akt phosphorylation (**B**) in HUVECs treated with SVP-CM. Data (means $\pm$ SE) are represented as fold changes to UCM from experiments performed in quadruplicates.  $\phi\phi$ P<0.01 vs. UCM;  $\phi$ P<0.05 and  $\phi\phi$ P<0.01 vs. corresponding group under normoxic SVP-CM;  $\#\#$ P<0.01 and  $\#\#\#$ P<0.001 vs. Scr.

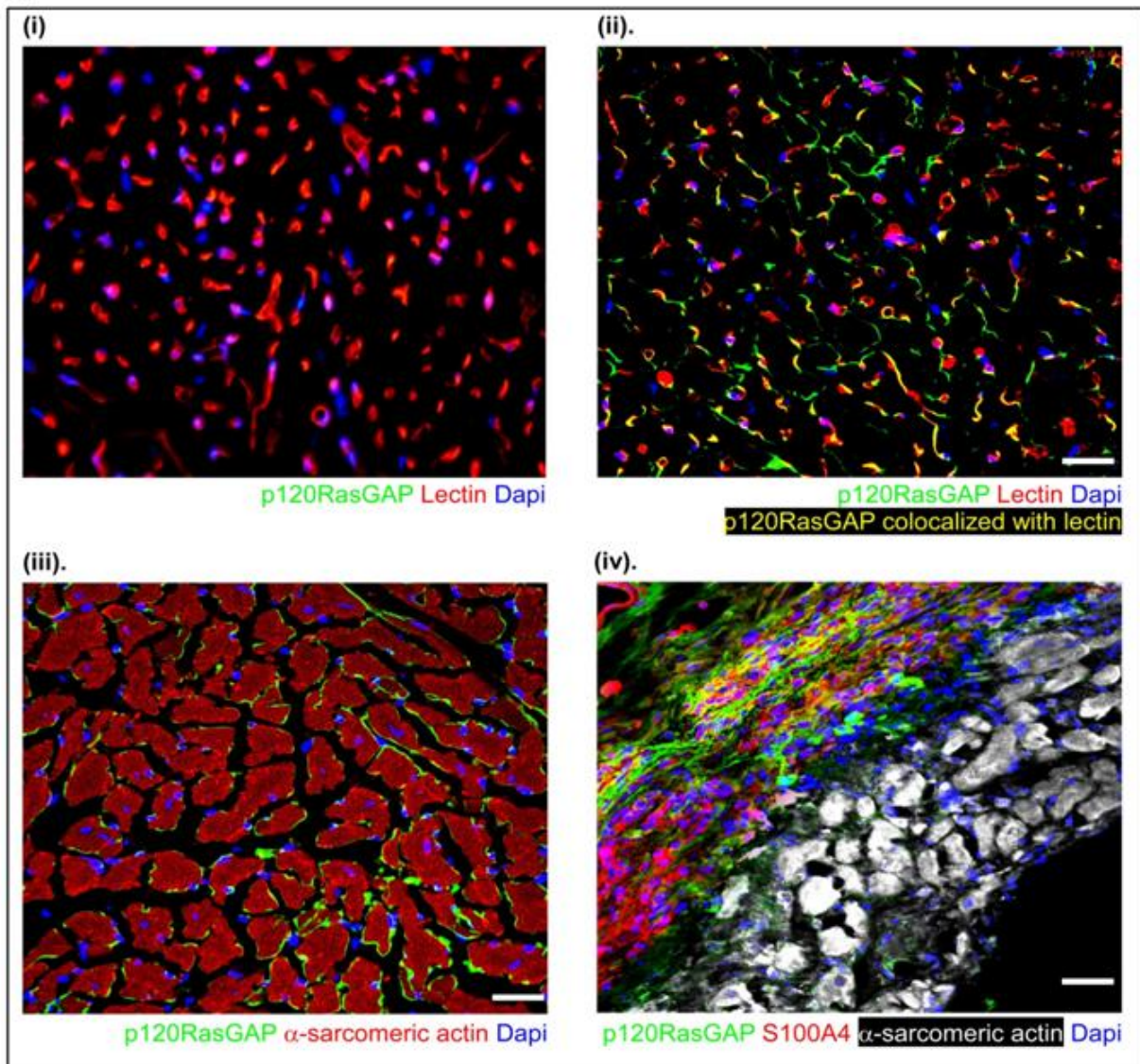




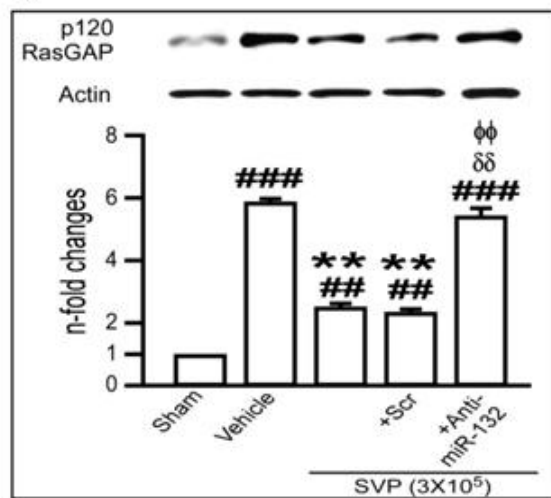
### Online Figure X

**A.** Bar graphs showing the level of angiogenic growth factors and miR-132 in SVP- and MSC-CM. Unconditioned medium (UCM) for SVPs is EB2 with 2% FBS and UCM for MSCs is mesenchymal stem cell media with 2% FBS and without growth factors. Data are means±SE. miR-132 levels are expressed as fold change vs. normoxic SVP-CM. \*\*P<0.01 vs. UCM; §P<0.05 and §§P<0.01 vs. normoxic CM; ###P<0.01 vs. SVP-CM under the same culture conditions. **B.** Representative images (i-vi) and bar graphs (vii) showing the network formation by HUVEC after treatment with UCM (i&iv) and SVP- (ii&iii) or MSC-CM (v&vi). Values are expressed as cumulative tube length per field and are means±SE. Experiments were performed in quadruplicates and repeated three times. Scale bars are 100µm. \*\*P<0.01 vs. UCM; ###P<0.001 vs. SVP-CM under the same culture conditions.

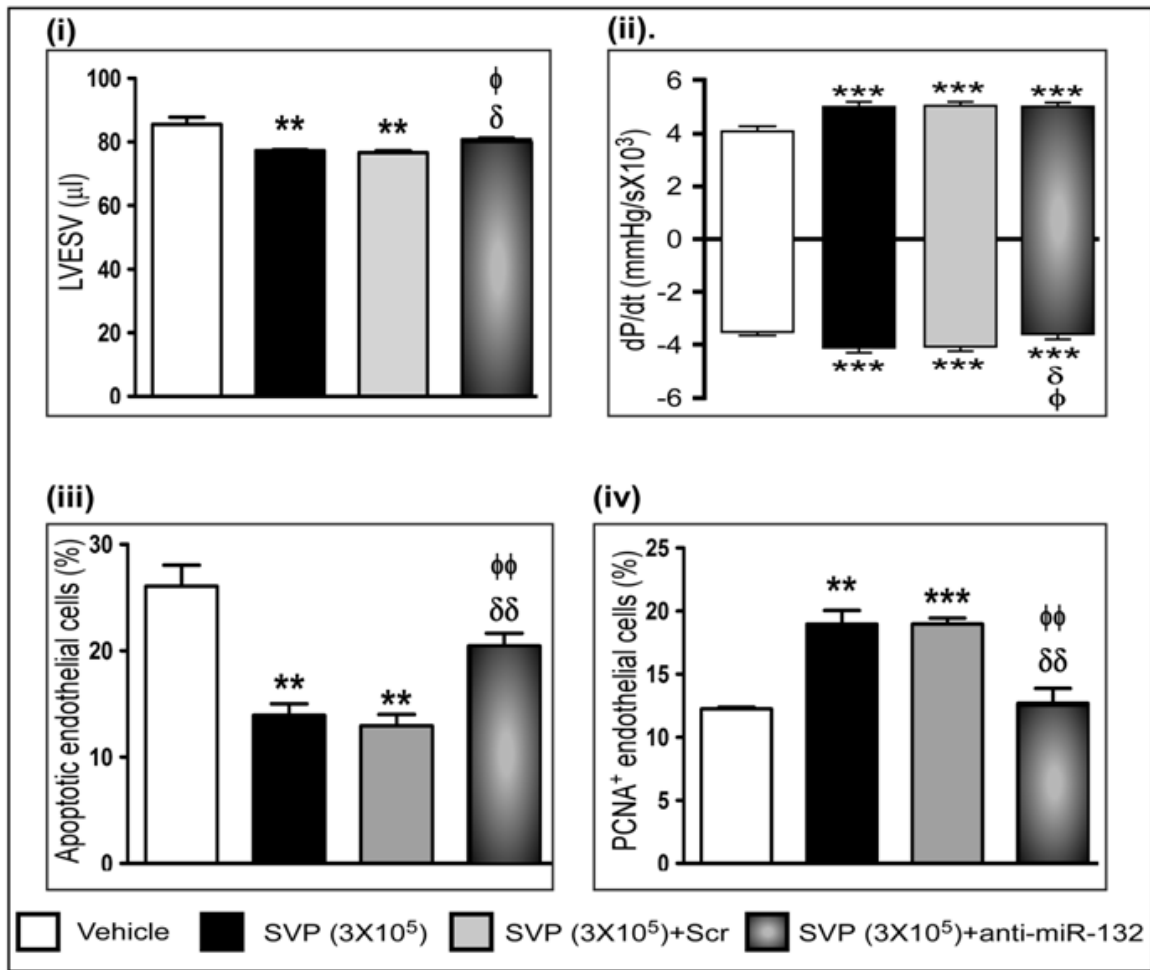
A.



B.

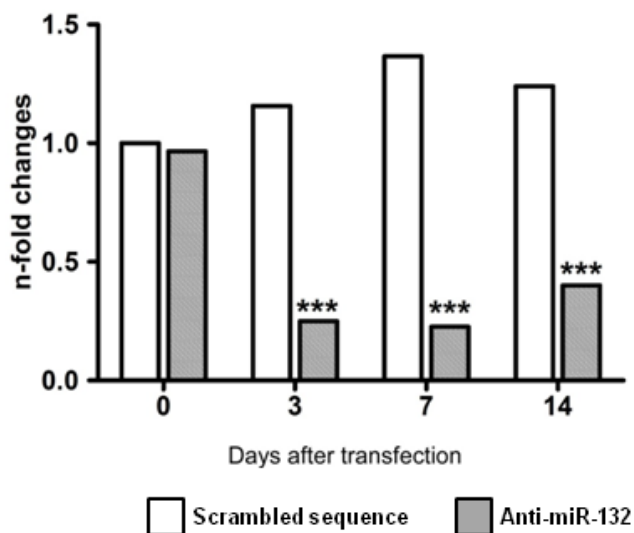


C.



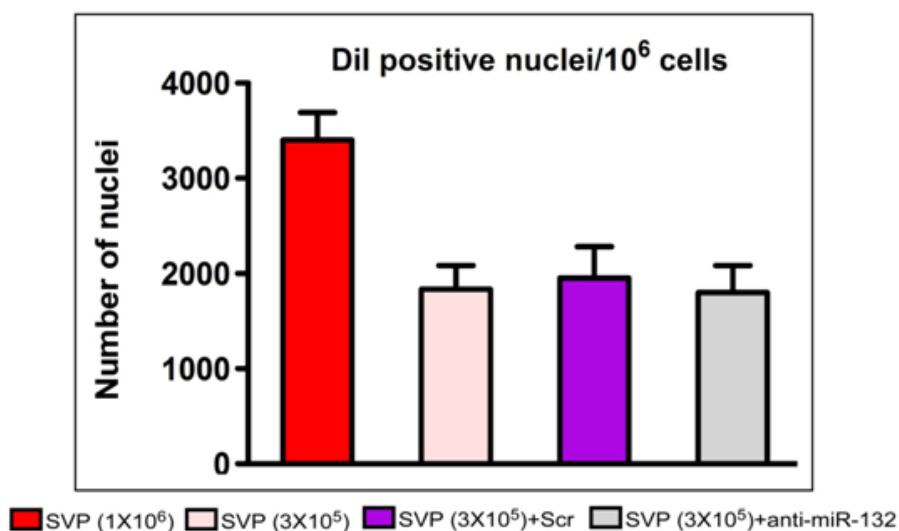
### Online Figure XI

**A.** Representative confocal images showing the localization of p120RasGAP in endothelial cells (ii), cardiomyocytes (iii) and fibroblasts (iv) in the myocardium at 14d post-MI. Negative control (i) without primary antibody to p120RasGAP was used as reference. Scale bars are 50μm. **B.** Representative western blots and bar graph showing the levels of miR-132 target gene p120RasGAP in myocardium. **C.** Bar graphs showing hemodynamic data (i&ii), EC apoptosis (iii) and proliferation (iv) at 14d post-MI. Data are means±SE (n=5 mice per group except for hemodynamic measurements which consisted of 6 mice). ##P<0.01 and ###P<0.001 vs. sham; \*\*P<0.01 and \*\*\*P<0.001 vs. vehicle; δP<0.05 and δδP<0.01 vs. non-transfected SVPs; φP<0.05 and φφP<0.01 vs. Scr-transfected SVPs.



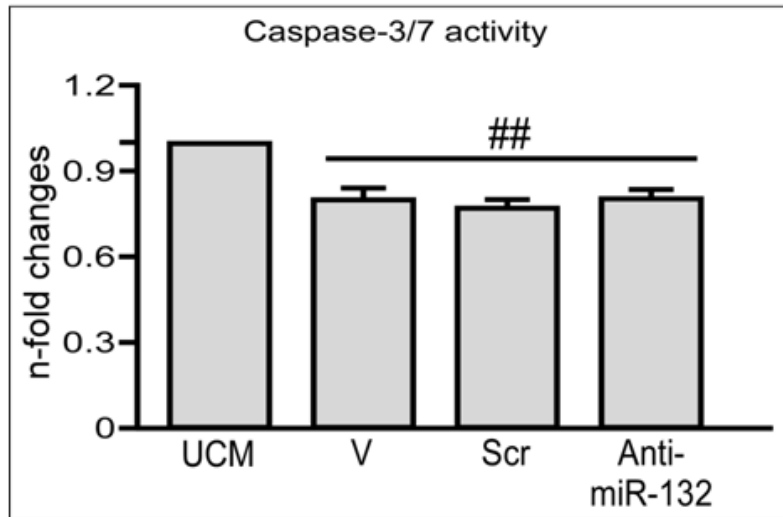
### Online Figure XII

Bar graphs showing long-term inhibition of miR-132 expression in SVPs transfected with anti-miR-132. Experiments were performed in triplicates. Data are means $\pm$ SE; \*\*\*P<0.001 vs. scrambled sequence.



### Online Figure XIII

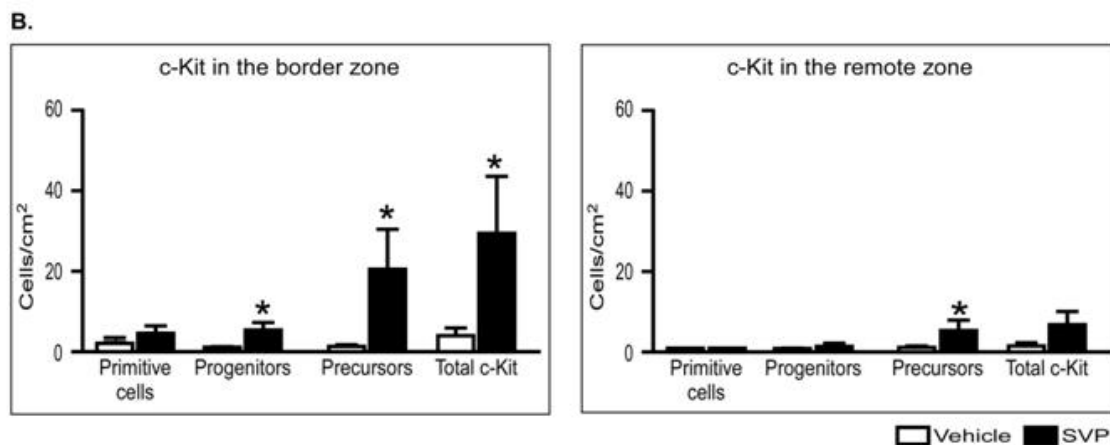
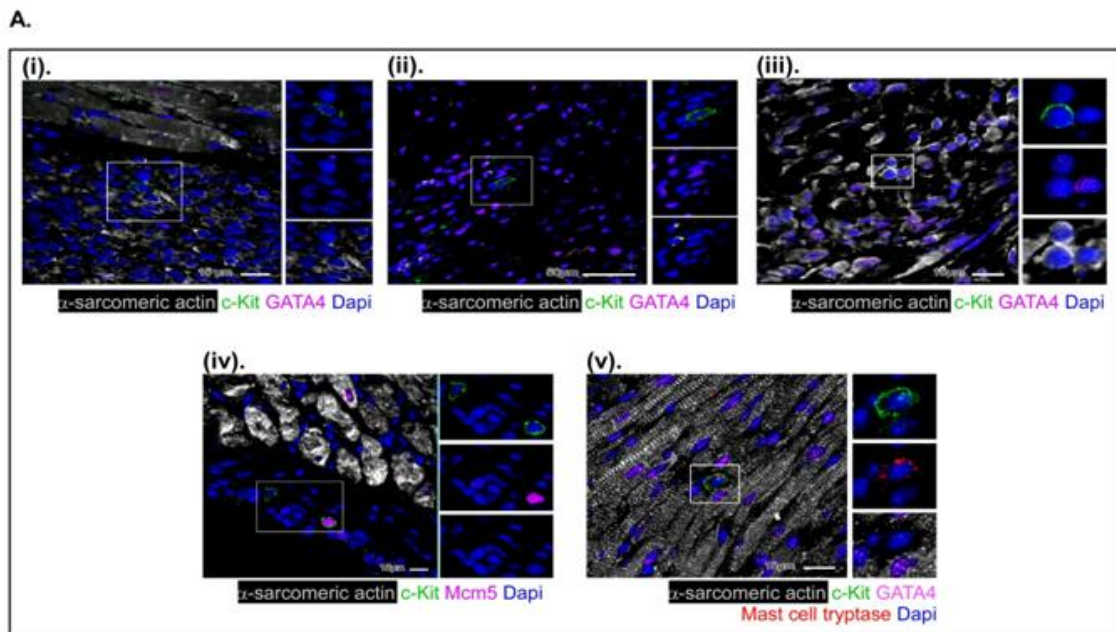
Bar graph showing the number of Dil-positive SVPs in the myocardium at 14d post-MI. Data expressed as number of Dil-positive cells per million cell nuclei and represented as means $\pm$ SE (n=6 mice per group).



**Online Figure XIV**

Bar graph showing caspase-3/7 activity in adult rat cardiomyocytes exposed to hypoxia after treatment with SVP-CM. Data are means $\pm$ SE from experiment performed in quadruplicate. ##P<0.01 vs. unconditioned medium (UCM).

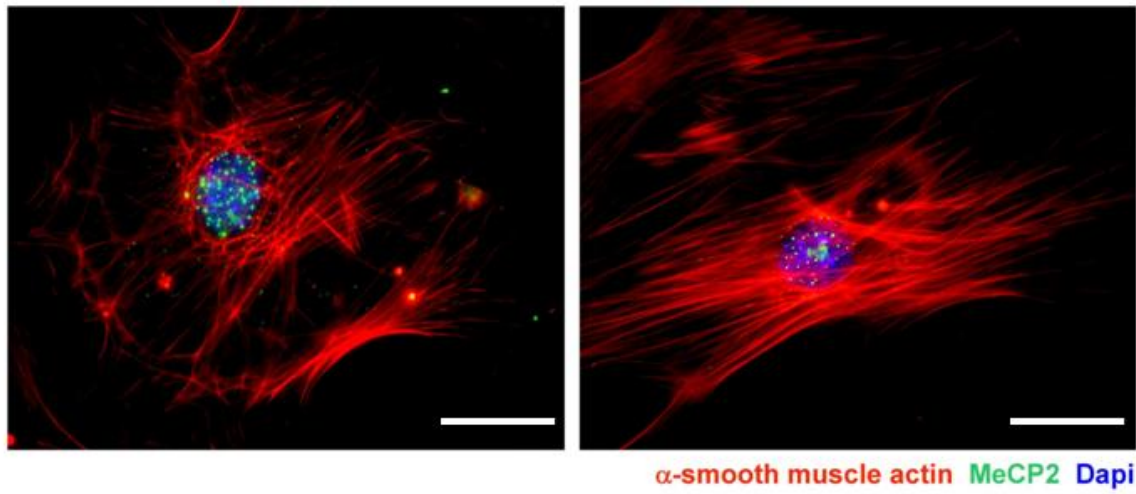




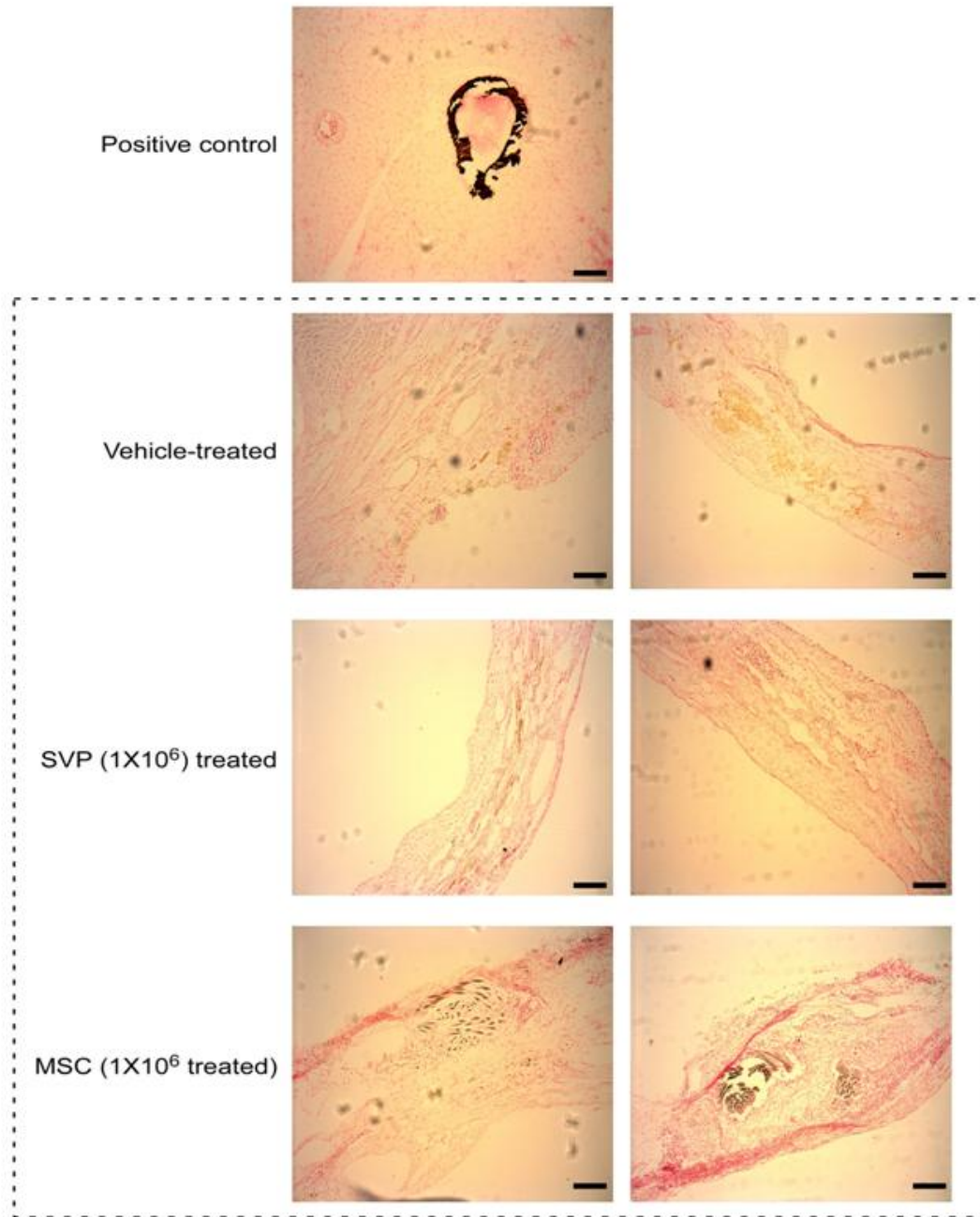
### Online Figure XV

**A.** Representative images showing different cardiac stem cell populations such as (i) primitive cells (c-Kit(+) GATA4(-) $\alpha$ -sarcomeric actin(-)), (ii) progenitors ((c-Kit(+))GATA4(+) $\alpha$ -sarcomeric actin(-)), (iii) precursors (c-Kit(+)) GATA4(+) $\alpha$ -sarcomeric actin(+)), (iv) proliferating c-Kit cells (c-Kit(+))Mcm5(+)  $\alpha$ -sarcomeric actin(-)) and (v) mastocytes (c-kit(+))Mast cell tryptase (+) GATA4(-) $\alpha$ -sarcomeric actin(-)) in the infarcted myocardium at 14 days post-MI. Resident stem cells are identified as the c-Kit positive cells negative for mast cell tryptase. Scale bars are 15 $\mu$ m except for (ii) which is 50 $\mu$ m. **B.** Bar graphs showing the quantification of different populations of cardiac stem cells at 14d post-MI. Data are means $\pm$ SE (n= 7 in vehicle and 9 in SVP treated group). \*P<0.05 vs. vehicle.





**Online Figure XVI.** Representative images showing Angiotensin-II differentiated myofibroblasts staining positive for  $\alpha$ -smooth muscle actin and MeCP2. Scale bars are 50 $\mu$ m.



**Online Figure XVII.** Representative microscopic images of Von Kossa staining in the infarct zone of the myocardium at 42d post-MI. Fibula of 3 weeks old mice was used as positive control. Two representative images are shown from each group. Scale bars are 100µm.